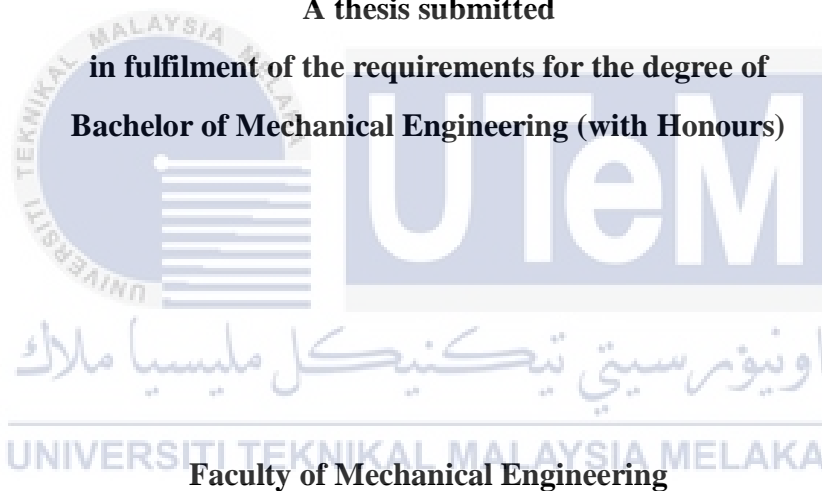


**EFFECT OF TENSILE TEST SPECIMEN GEOMETRY ON MECHANICAL
PROPERTY OF 3D PRINTED SINGLE STRUTS**

AZIRA BINTI MAT YUSOF

A thesis submitted

**in fulfilment of the requirements for the degree of
Bachelor of Mechanical Engineering (with Honours)**



Faculty of Mechanical Engineering

UNIVERSITI TEKNIKAL MALAYSIA MELAKA

2019

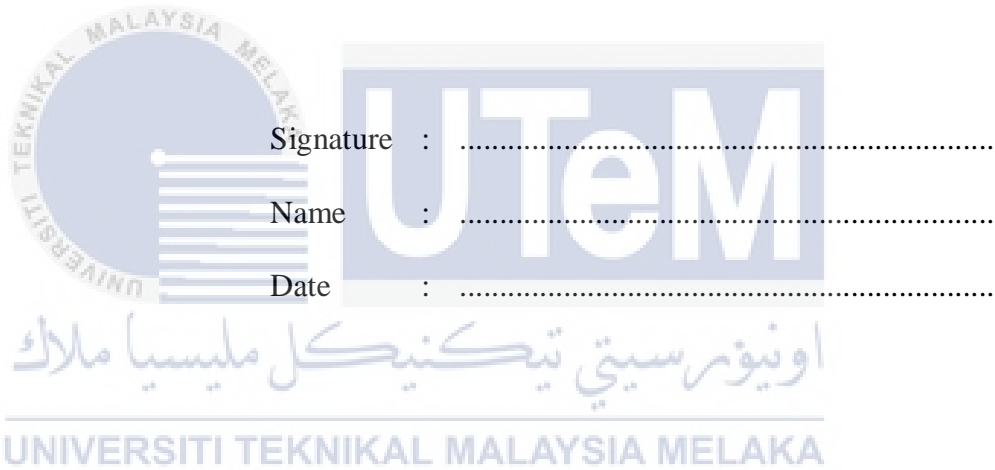


اونيورسيتي تيكنيكل مليسيا ملاك

UNIVERSITI TEKNIKAL MALAYSIA MELAKA

DECLARATION

I declare that this project report entitled “Effect of Tensile Test Specimen Geometry on Mechanical Property of 3D Printed Single Struts” is the result of my own work except as cited in the references.



Signature :

Name :

Date :

اونيورسيتي تيكنيكل مليسيا ملاك

UNIVERSITI TEKNIKAL MALAYSIA MELAKA

APPROVAL

I hereby declare that I have read this project report and in my opinion this report is sufficient in terms of scope and quality for the award of the degree of Bachelor of Mechanical Engineering (with Honours).

Signature :

Name of Supervisor : DR. RAFIDAH BINTI HASAN

Date :



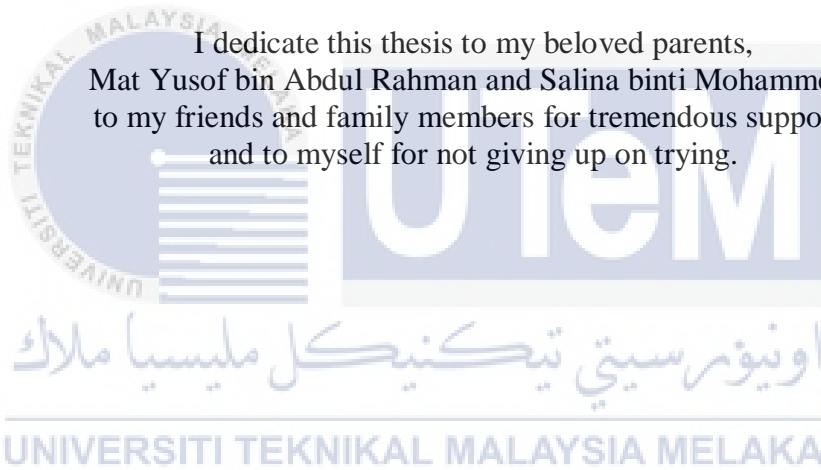
اونيورسيتي تيكنيكل مليسيا ملاك
UNIVERSITI TEKNIKAL MALAYSIA MELAKA

DEDICATION

“Nostalgia is like a grammar lesson. You find the present tense and past perfect”

- Orben’s comedy Fillers

I dedicate this thesis to my beloved parents,
Mat Yusof bin Abdul Rahman and Salina binti Mohammed;
to my friends and family members for tremendous supports
and to myself for not giving up on trying.



ACKNOWLEDGEMENT

First, I would like take this opportunity to express my greatest gratitude to my supervisor, Dr. Rafidah binti Hasan, for guiding me throughout this project with patience, encouragement and supports. All the knowledge that I gained enable me complete this final year project successfully.

Next, I would like to express my appreciation to Dr. Mohd Basri bin Ali and Dr Mohd Azli bin Salim as my panel seminar. For all the knowledge shared during seminar that had helped me a lot to improve my thesis.

Lastly, I would like to thank Universiti Teknikal Malaysia Melaka (UTeM) especially Faculty of Mechanical Engineering (FKM) for giving fully support by allowing me to use their equipment and facilities during conducting my study.



ABSTRACT

The lattice-structure material is a light-weighted material which suitable for lightweight structural application. Elementary unit of lattice structure is single strut which connects two nodes. It is important to know mechanical properties of single strut as they contribute to lattice structure performance. Elastic property is one of the mechanical properties which can be obtained through tensile test. Best elastic property data comes from suitable tensile test specimen geometry. This study is conducted to determine the specimen geometry effect on elastic property of tensile test for acrylonitrile butadiene styrene (ABS) 3D printed single strut specimen. Single struts with geometrical shape (Dogbone) and without geometrical shape (Cylinder) are designed by using a CAD software which is Solidworks. Then, single struts are fabricated by using CubePro 3D printer. Next, tensile test is conducted to single strut specimens. From tensile test, data on Young's modulus is established. Furthermore, hypothesis test is applied on the Young's modulus data to verify the theory made. The engineering conclusions are concluded from hypothesis test on specimen geometry effect on elastic property of tensile test for ABS 3D printed single strut specimen.

اونيورسيتي تيكنيكل مليسيا ملاك

UNIVERSITI TEKNIKAL MALAYSIA MELAKA

ABSTRAK

Kekisi-struktur bahan adalah bahan ringan yang sesuai bagi aplikasi struktur ringan. Unit asas struktur kekisi adalah tupang tunggal yang menghubungkan dua nod. Ia adalah penting untuk mengetahui sifat-sifat mekanik tupang tunggal kerana mereka menyumbang kepada prestasi struktur kekisi. Sifat keanjalan adalah salah satu daripada sifat-sifat mekanikal yang boleh diperolehi melalui ujian tegangan. Data sifat keanjalan yang terbaik datang dari geometri spesimen ujian tegangan yang sesuai. Kajian ini dijalankan untuk menentukan kesan geometri spesimen ke atas sifat keanjalan bagi spesimen ujian tegangan bagi acrylonitrile butadiene styrene (ABS) 3D tupang tunggal bercetak. Tupang tunggal dengan bentuk geometri (Dogbone) dan tanpa bentuk geometri (silinder) direka dengan menggunakan perisian CAD ia itu Solidworks. Kemudian, tupang tunggal dihasilkan dengan menggunakan pencetak 3D CubePro. Seterusnya, ujian tegangan dijalankan ke atas spesimen tupang tunggal. Dari ujian tegangan, data modulus Young akan dihasilkan. Selain itu, ujian hipotesis digunakan kepada data modulus Young bagi mengesahkan teori yang telah dibuat. Kesimpulan kejuruteraan akan dihasilkan daripada ujian hipotesis bagi menguji adakah geometri spesimen memberi kesan ke atas sifat keanjalan bagi spesimen ujian tegangan tupang tunggal ABS 3D bercetak.

TABLE OF CONTENTS

DECLARATION		ii
APPROVAL		iii
DEDICATION		iv
ACKNOWLEDGEMENT		v
ABSTRACT		vi
ABSTRAK		vii
TABLE OF CONTENTS		viii
LIST OF FIGURES		x
LIST OF TABLES		xiii
LIST OF ABBREVIATIONS		xiv
LIST OF SYMBOLS		xv
CHAPTER		
1.	INTRODUCTION	
	1.1 Background	1
	1.2 Problem statement	3
	1.3 Objective	3
	1.4 Scope of Project	4
2.	LITERATURE REVIEW	
	2.1 Introduction	5
	2.2 Lattice-structure and strut	5
	2.3 Methods in Producing Lattice Structure	6
	2.4 Additive Layer Manufacturing	9
	2.5 Polymer 3D Printer	10
	2.6 Comparative Experiment	11
	2.7 Hypothesis test	12
	2.8 Tensile test	13
3.	METHODOLOGY	
	3.1 Introduction	17
	3.2 Workflow Chart	17
	3.3 Design Stage	19
	3.4 Fabrication Stage	25
	3.5 Tensile test	28
	3.6 Hypothesis Test	30
	3.6.1 Testing of Variances (F-Test)	32
	3.6.2 Comparison of Means (T-Test)	35
4.	RESULT AND DISCUSSION	
	4.1 Introduction	38
	4.2 Design stage	38

4.3	Tensile test	41
4.4	Analysis	43
4.4.1	Young's modulus for Cylinder and Dogbone1	44
4.4.2	Young's modulus for Cylinder and Dogbone2	52
5.	CONCLUSION AND RECOMMENDATION	
5.1	Conclusion	65
5.2	Recommendation	66
	REFERENCES	67



LIST OF FIGURES

FIGURE	TITLE	PAGE
1.1	Lattice structure with different lattice arrangements	2
2.2	Struts and nodes based lattice arrangement, n=9 and p=16	6
2.3.1	Lattice structure assembled to be 3D Kagome core sandwich panel	7
2.3.2	Deformation of sheet metal forming process	8
2.4	Schematic of Selective Laser Melting process	10
2.5	CubePro 3D printer	11
2.6	Means formula	12
2.7	Flow of Hypothesis test	13
2.8.1	Stress-strain graph of well-aligned sample for tensile testing of micro sample	15
2.8.2	The stress-strain graph of 7075 aluminium alloy tensile test specimen	16
2.8.3	Stress-strain graph for AA7075 aluminium alloy specimen after tensile test was done	16
3.2	Flowchart of methodology	18
3.3.1	The standard measurement for tensile test specimen for metal	19
3.3.2	The part drawing of Cylinder single struts using Solidworks	22
3.3.3	The part dimension drawing of Cylinder single struts using Solidworks	22
3.3.4	The part drawing of Dogbone1 (0.90 mm fillet radius) single struts using Solidworks	23
3.3.5	The part dimension drawing of Dogbone1 (0.90 mm fillet radius) single struts using Solidworks	23
3.3.6	The part drawing of Dogbone2 (0.48 mm fillet radius) single struts using Solidworks	24

3.3.7	The part dimension drawing of Dogbone1 (0.48 mm fillet radius) single struts using Solidworks	24
3.4.1	Build settings of CubePro software	26
3.4.2	Descriptions on the build settings	26
3.4.3	Single struts with slices in CubePro software	27
3.4.4	Parameters selected for both dogbone and cylinder single strut	28
3.5.1	Shimadzu EZ Test (EZ-LX) test machine	29
3.5.2	Trapezium X software window	29
3.5.3	Graph to find Young's modulus	30
3.6.1	Flow of hypothesis test.	32
4.2.1	Stress-concentration factor, k_t for a filleted shaft in tension	39
4.2.2	Design with dimension for single strut specimen with geometrical shape, Dogbone1 (0.90 mm fillet radius)	39
4.2.3	Design with dimension for single strut specimen with geometrical shape, Dogbone2 (0.48 mm fillet radius)	40
4.2.4	Design with dimension for single strut specimen without geometrical shape, Cylinder	40
4.3.1	Stress-strain graph of dogbone single strut specimen for 0.9mm fillet radius (single strut specimen with geometrical shape), Dogbone1	41
4.3.2	Stress-strain graph of dogbone single strut specimen for 0.48mm fillet radius (single strut specimen with geometrical shape), Dogbone2	42
4.3.3	Stress-strain graph of cylinder single strut specimen (single strut specimen without geometrical shape)	42
4.4.1.1	Bell graph for variance at 5% significant level for Cylinder and Dogbone1 (0.9mm radius fillet)	49
4.4.1.2	Bell graph for Young's modulus of Cylinder and Dogbone1 (0.9mm radius fillet) t-TEST	52
4.4.2.1	Bell graph for variance at 5% significant level for Cylinder and Dogbone2 (0.48 mm radius fillet)	58



LIST OF TABLES

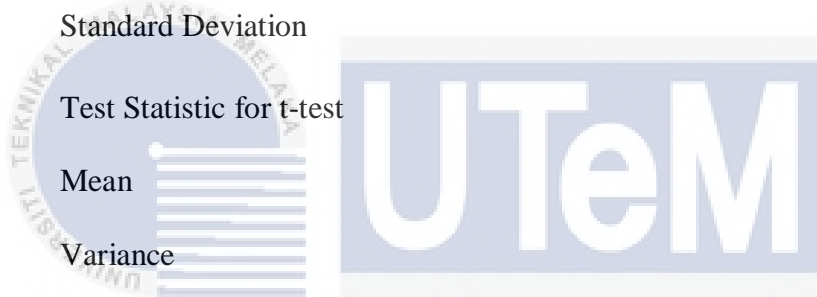
TABLE	TITLE	PAGE
3.3.1	Details on single strut specimen for tensile test	20
3.6.1	Process parameters selected in CubePro 3D printer	31
4.3.1	Young's modulus values for cylinder and dogbone single struts	43
4.4.1.1	Summation on means of Young's modulus for single strut specimen without geometrical shape (Cylinder) F-TEST, S1	45
4.4.1.2	Summation on means of Young's modulus for single strut specimen with geometrical shape (Dogbone1) F-TEST, S2	47
4.4.2.1	Summation on means of Young's modulus for single strut specimen without geometrical shape (Cylinder) F-TEST, S1	54
4.4.2.2	Summation on means of Young's modulus for single strut specimen with geometrical shape (Dogbone2) F-TEST, S2	56
4.4.2.3	Distribution graph for hypothesis test	62
4.4.2.4	Average Young's modulus mean for single strut specimen with and without geometrical shape	63

LIST OF ABBEREVATIONS

3D	3 Dimensional
ABS	Acrylonitrile Butadiene Styrene
AM	Additive Manufacturing
ALM	Additive Layer Manufacturing
ASTM	American Society of Testing for Material
BCC	Body-Centred-Cubic
FCC	Face-Centred-Cubic
FDM	Fused Deposition Modeling
CAD	Computer-Aided Design
HCP	Hexagonal Close Packed
PLA	Polylactic Acid
SLM	Selective Laser Melting
STL	Standard Tessellation Language

LIST OF SYMBOLS

α	=	significant level
DF	=	Degree of Freedom
H_0	=	Null hypothesis
H_A	=	Alternative hypothesis
F	=	Test Statistic for F-test
n	=	Number of Sets
S	=	Standard Deviation
t	=	Test Statistic for t-test
μ	=	Mean
σ	=	Variance



اونيورسيتي تيكنيكل مليسيا ملاك
UNIVERSITI TEKNIKAL MALAYSIA MELAKA

CHAPTER 1

INTRODUCTION

1.1 Background

The production of lattice structures by using additive manufacturing (AM) in recent years is increasing as more and more studies have shown the potential of using this material in many application such as energy absorber, acoustic absorber and thermal insulator (Kilinc et al., 2016; Tan et al., 2019; Davami et al., 2019; Mohsenizahed et al., 2017; Guild et al., 2015). Now, studies proved that open-pored cellular lattice structures with more complex geometrical structures are able to be created compared to the starting of the decade where the structures are mostly in regular rectangular forms (Rehme and Emmelmann, 2006).

Lattice structure material is a material which is lightweight, with the properties of high stiffness and strength-to-weight scaling (Doyoyo and Hu, 2006). Many studies have been done to determine the mechanical properties of this material including stainless steel, aluminium, titanium alloy and few other metals. Single strut is the elementary unit of this lattice structure material. The availability of the joint type makes the assembly methods of the strut-based lattice structure to be a flexible configuration which is preferred for complex geometrical designs (Doyoyo and Hu, 2006).

Lattice structure comprises of many struts connected to each other by nodes, in many architectural arrangements such as body-centred-cubic (BCC), face-centred-cubic (FCC) and hexagonal close packed (HCP) (Mines, 2008). A lot of possible architectural arrangements can be proposed within an outlined volume as lattice structure composed of

numerous number of nodes and struts. An example of lattice structure with different arrangements is shown in Figure 1.1 (Syam et al., 2017).

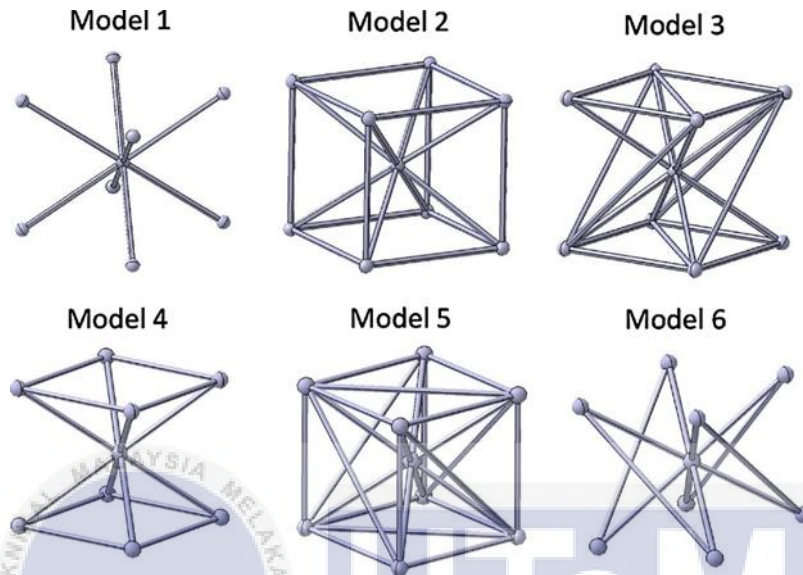


Figure 1.1: Lattice structure with different lattice arrangements
(Source: Syam et al., 2017)

The value for mechanical properties, the performance and the quality of lattice structure can be concluded through examination of struts, thus making struts as fundamental entity for lattice structure (Kessler et al., 2016). Studies have shown that different geometric shapes will affect various mechanical properties, as they are closely related to shear band process and deformation process constrain (Calik et al., 2008). Therefore, this research will observe on struts with and without geometric shape to assist better understanding on how geometric shape affects mechanical properties for lattice structure.

1.2 Problem statement

Tension, compression and flexure are important aspects that need to be fully characterized in lattice- structure material study to know its optimum functionality and mechanical properties. Based on previous research (Wahi, 2018), compression test was done for 3D printed polymer lattice structure; acrylonitrile butadiene styrene (ABS) material specimen, with and without enhancement of lattice structure unit, to get the compression stress versus compression strain diagram in providing information on mechanical properties particularly on young modulus, yield strength and maximum strength of lattice structure materials. However, this compression test is unable to give data on failure strength or failure strain which can be attained through tensile test. When it comes to obtain failure data, tensile test is preferable. To simplify this, it is suggested that tensile test on single strut specimen for ABS material to be performed in providing information related to basic failure of lattice structure material. Best elastic property data comes from suitable tensile test specimen geometry. In order to get precise information from the tensile test, it is important to study the proper handling of single strut specimen which is affected by the geometric shape of the specimen. Thus, this study is to determine the specimen geometry effect on elastic property of tensile test for ABS 3D printed single strut specimen.

1.3 Objective

The objective of this study is to investigate the effect of geometric shape on elastic property of tensile test for 3D printed single strut with selected parameter.

1.4 Scope of Project

The scopes of this project are:

- i. Design single strut with and without geometrical shape by using acrylonitrile butadiene styrene (ABS) material for tensile test specimen referring to ASTM (E8/E8M-13a) for the specimen design ratio.
- ii. Use a CAD software which is Solidworks to design and CubePro 3D printer to fabricate both type of single struts.
- iii. Use Shimadzu EZ Test (EZ-LX) machine to conduct tensile test for both type of single struts.



CHAPTER 2

LITERATURE REVIEW

2.1 Introduction

The background of this chapter is based on relevant journal articles and academic books that are related to this study. It is needed for this chapter to be studied for better understanding for the next progress as this chapter describes on previous studies that related to this study.

2.2 Lattice-structure and strut

Lattice structure material is a material which is lightweight structure with the properties of high stiffness and strength-to-weight scaling (Doyoyo and Hu, 2006). Many studies have been done to determine the mechanical properties of this material including stainless steel, aluminium, titanium alloy and few other metals. Single strut is the elementary unit of this lattice structure material. The availability of the joint type makes the assembly methods of the strut-based lattice structure to be a flexible configuration which is preferred for complex geometrical designs (Doyoyo and Hu, 2006).

Lattice structure comprises of many strut connected to each other by nodes, in many architectural arrangements such as body-centred-cubic (BCC), face-centred-cubic (FCC) and hexagonal close packed (HCP) (Mines, 2008). A lot of possible architectural arrangements can be proposed within an outlined volume as lattice structure composed of numerous number of nodes and struts. An example of lattice structure with its nodes (n) and struts (p) is shown in Figure 2.2 (Syam et al., 2017).

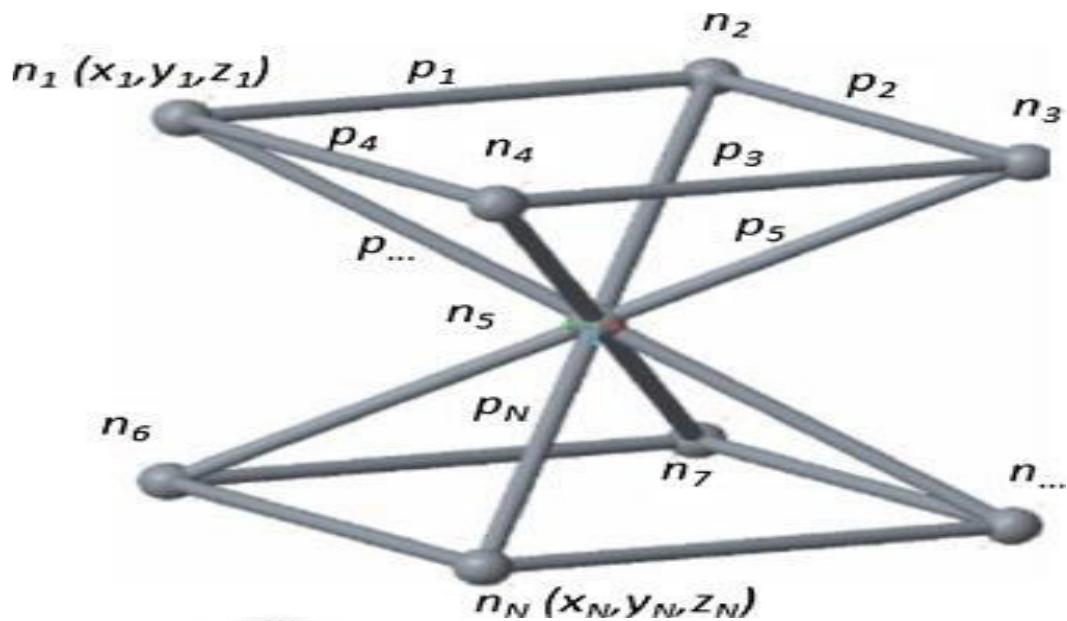


Figure 2.2: Struts and nodes based lattice arrangement, $n=9$ and $p=16$

(Source: Syam et al., 2017)

2.3 Methods in Producing Lattice Structure

There are conventional and advanced method in manufacturing lattice-structures. Conventionally, lattice-structures are manufactured through casting, sheet metal forming or wire bonding process. These traditional manufacturing process are time-consuming and limiting lattice structure with complex designs to be built (Rashed et al., 2016).

For investment casting process (Rashed et al., 2016), a volatile wax or polymer is injected from an injection molding or a rapid prototyping to manufacture the truss pattern. This is where the system of gating and risers will be used to coat pattern by ceramic casting slurry. The wax or polymer is then detached by melting or vaporization process, followed by contenting metal liquid into the empty mold. The weakness of this method is that this method is pricey and taking more time to be manufactured. The structures manufactured also contained considerable porosity. Figure 2.3.1 shows the example of lattice material that is

manufactured through investment casting process and has been assembled to be 3D Kagome core sandwich panel.

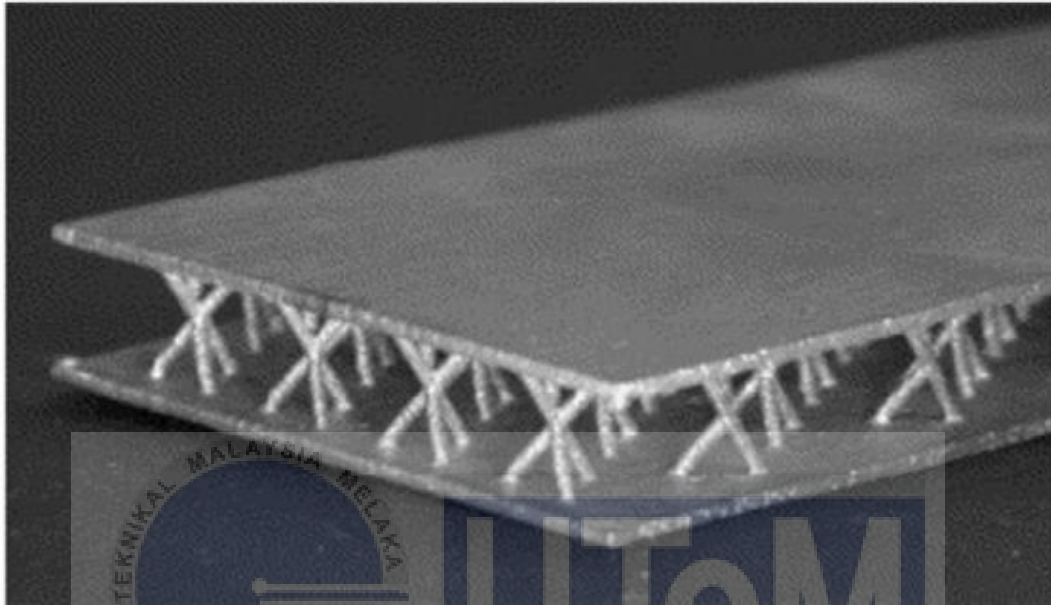


Figure 2.3.1: Lattice structure assembled to be 3D Kagome core sandwich panel

(Source: Rashed et al., 2016)

For sheet metal forming method (Rashed et al., 2016), press forming operation is used to produce lattice structure. This method enable cell sizes of millimeter to several centimeters to be obtained as it utilizes the usage of sheet perforation and shaping techniques. The perforated metal sheets are deformed with hexagonal or diamond shaped holes at the nodes and assembled to produce different sheets of structure such as tetrahedrons or pyramidal. Figure 2.3.2 shows deformation of sheet metal forming process.

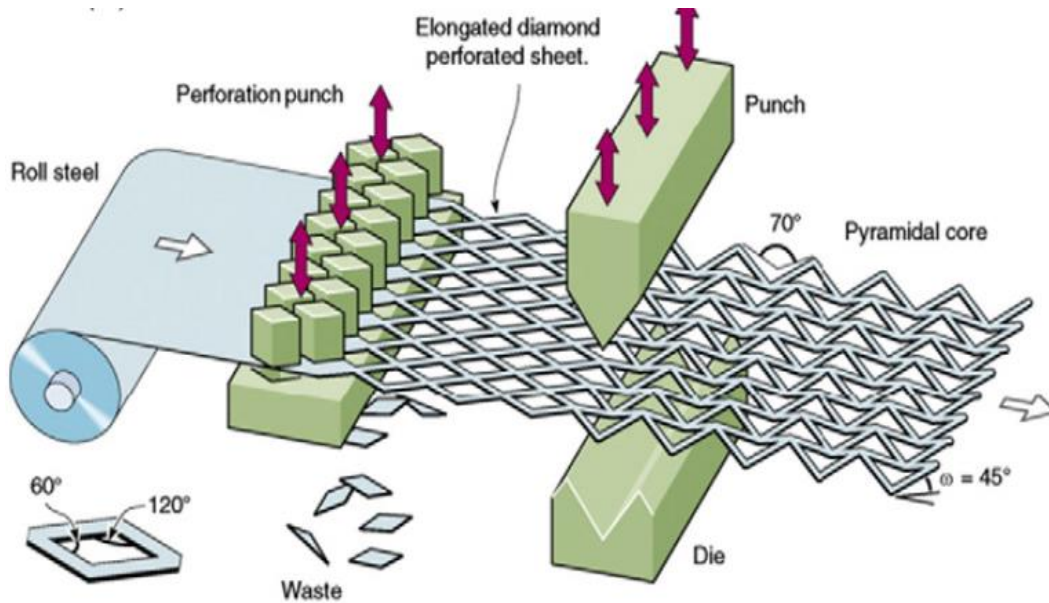


Figure 2.3.2: Deformation of sheet metal forming process

(Source: Rashed et al., 2016)

For wire bonding process (Rashed et al., 2016), the method is limited to produce metal lattice structures. This method is relatively faster compared to other method but it is not effective as it caused wastage of material throughout the making process. This method promises a good surface quality.

The introduction of additive manufacturing (AM) technologies in advance manufacturing is a very helpful discovery. Producing lattice structures by using AM technologies had reduced many limitations that is countered in conventional manufacturing process. Highly complex components with inside-lying structures and functional areas can be manufactured through one process step. This has made AM technologies less time consuming as compared to conventional manufacturing technologies (Kessler et al., 2016).

2.4 Additive Layer Manufacturing

In recent years, studies have been focused more on the development of lattice structure material application. The application of lattice structure are widely used in various application with the advent of Additive Layer Manufacturing (ALM) (Augustyniak, 2017). ALM has make lattice structure material with length scales of millimeters are able to be assembeled (Yan et al., 2012).

There are steps to assemble lattice structure material by using Additive Manufacturing (AM) technology. Usually, the first process of AM technology is to design and build a 3D modeling by using Computer-Aided Design (CAD) software. Then, the drawing from CAD software will be converted into “STL” (Standard Tessellation Language). This STL file is to create slices from the model for data preparation. Next, data is used to produce designed models. This is by inserting data into a program of an AM machine. Removing support structure or surface finishing is needed during post processing (Kessler et al., 2016).

One of AM techniques is Selective Laser Melting (SLM). SLM is a powder-based AM technology and its raw material used is metal powder. The principle of this process is that a very thin layers of metal powder is applied on building platform. The thin layers of metal powder is then completely melted by using thermal energy induced by laser beam and re-solidified to produce the designed part (Rashed et al., 2016). SLM is a method that avoids wastage of material as laser beam will follow computer-generated pattern which can be redirected and focused across powder bed when detected by scanner optics (Rashed et al., 2016). Although any arbitrary shape can be produced as the fabrication process is a freeform, SLM process has its own limitations. Overhanging geometries are difficult to be produced due to poor heat conduction in the powder bed below new laid exposed powder. Horizontal

struts are also difficult to be produced (Rehme and Emmelmann, 2006). Figure 2.4 shows the schematic of SLM process.

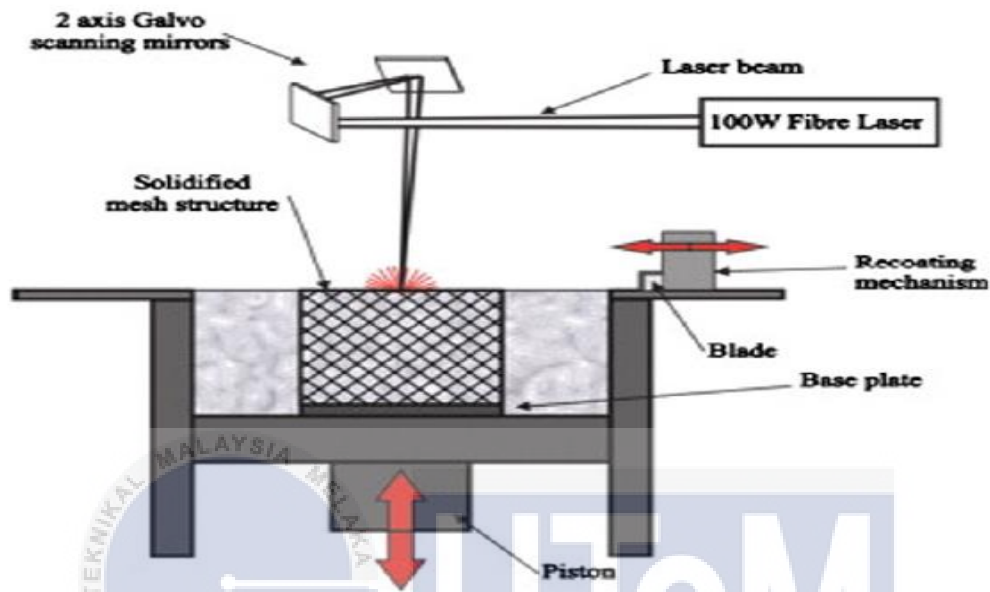


Figure 2.4: Schematic of Selective Laser Melting process

(Source: Tsopanos et al., 2010)

2.5 Polymer 3D Printer

In this study, Fused Deposition Modeling (FDM) method is used to fabricate strut formations by using 3D printer. Semi- liquid material is extruded through melted plastic material which is in filament form. The extruded material is then solidified and built layer-by-layer to form the model. Few parameters such as material strength, deposition speed, layer thickness and envelope temperature can affect the performance and functionalities of the system (3dsystems, 2017).

For this study, the 3D printer chosen is CubePro Printer. There are few specifications feature in CubePro printer. The ultra-high-resolutions setting of the printer are 70 microns,

200 microns and 300 microns thin print layers. The operating temperature at extruder tip is up to 280°C and the maximum deposition speed is 15mm per second. The printer has a good accuracy for model printing as it features Z axis resolution of 0.1mm. PLA (polyactic acid) or ABS (acrylonitrile butadine styrene) is material used for this printer (3dsystems, 2017). Figure 2.5 shows a CubePro printer available at Prototyping and Innovation laboratory in Universiti Teknikal Malaysia Melaka that has been used to print the struts.

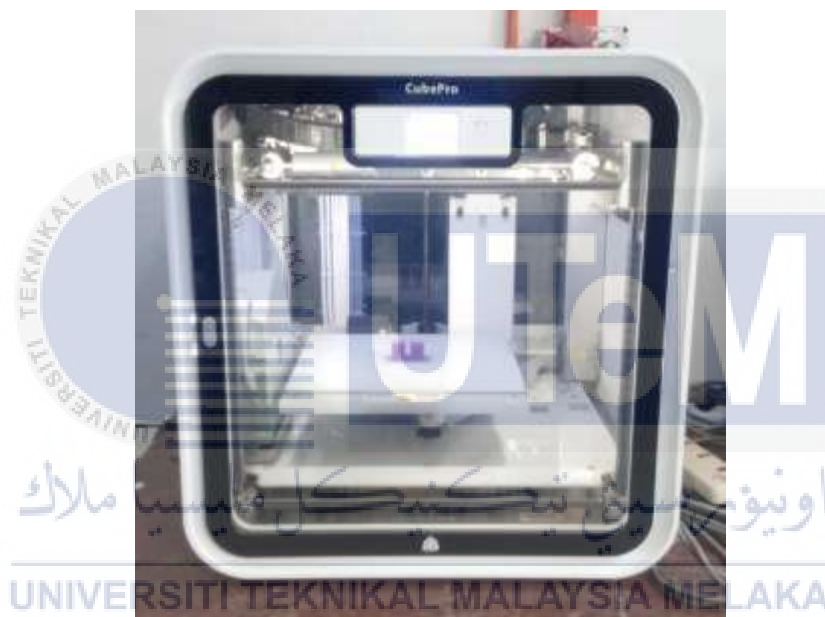


Figure 2.5: CubePro 3D printer

2.6 Comparative Experiment

Comparative experiment is an experimental design method in which two or more samples exposed to different conditions or treatments and are compared to each other (Statics in Plain English, 2010). This could be in terms of different processes, methods, materials or even operator. The purpose of comparative experiment is to determine if there is any significant difference between data collected. Figure 2.6 shows the terms that are needed to be understood in doing comparative experiment. Mean is simply arithmetic average of a

distribution of scores. Mean is divided into two sections. They are population mean and sample mean. Population is a group which data is collected while sample is an individual or group selected from population which data is collected (Timothy, 2010).

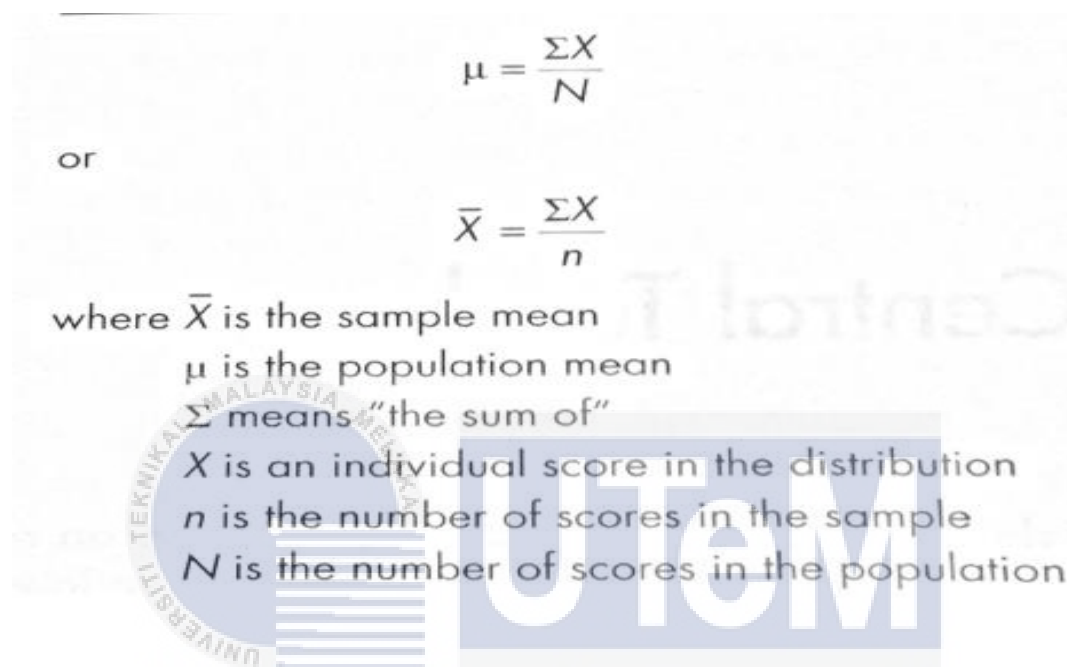


Figure 2.6: Means formula

(Source: Timothy, 2010)

2.7 Hypothesis test

Hypothesis test is one of the comparative experiments. Data will be analysed by using hypothesis test where the theory is confirmed by using information from the data (Kuang, 2007). Null hypothesis (H_0) is the assumption that data is kept the same while alternative hypothesis (H_0 and H_A) is a theory that will be tested. A condition of rejecting the (H_0) is when the level changes within 1% to 5%. The comparison of means which is called as t-test needs to be done when conducting hypothesis test, followed by testing of variance called F-test. Figure 2.7 shows the flow of hypothesis test which is conducted by (Kuang, 2007).

FLOW OF HYPOTHESIS TEST

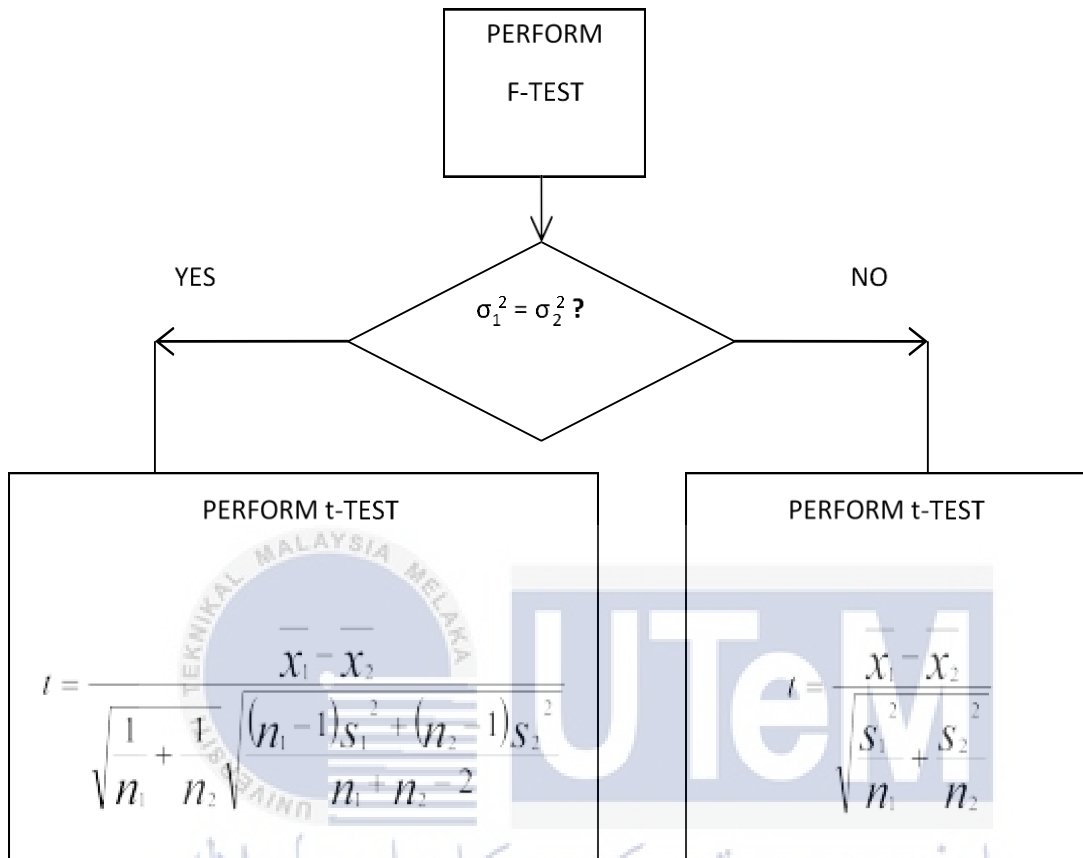


Figure 2.7: Flow of Hypothesis test

(Source: Kuang,2007)

2.8 Tensile test

There are several purpose of tensile test to be performed. When selecting materials for engineering applications, tensile test results are used where tensile properties are included in material specifications to ensure quality. Tensile test properties are often measured during development of new materials or processes so that different materials and processes can be compared (Tensile Testing, 2nd Edition, 2004).

Lately there are many research projects that have been carried out on Additive Manufacturing (AM) (Kessler et al., 2016). 3D printing which is one of AM method is included. 3D printed products are usually tested for their mechanical properties. One of a way in getting this mechanical properties is by conducting tensile test. From tensile test data results, Stress-Strain graph can be plotted and mechanical properties such as yield strength and Young's Modulus can be acquired (Tensile Testing, 2nd Edition, 2004).

There are studies conducted which are related to tensile test (LaVan and Sharpe, 1999; Chen, You and Gao, 2014; Kumar, Reddy and Rao, 2015). There are examples on tensile test study that has been done such as tensile testing for microsamples (LaVan and Sharpe, 1999), analysis and experiment of 7075 aluminum alloy tensile test and the effect of post weld heat treatment on microstructure test (Chen, You and Gao, 2014) and mechanical and corrosion behavior of high strength AA7075 aluminium alloy friction stir welds (Kumar, Reddy and Rao, 2015). These studies are providing data that is converted to stress-strain graph for their mechanical properties to be analysed.

The first study is a tensile testing for microsamples (LaVan and Sharpe, 1999). The study showed a new system developed to conduct tensile test for microsample specimen. The result in the form of stress-strain graph are shown in Figure 2.8.1.

The second study is the analysis and experiment of 7075 aluminum alloy tensile test (Chen, You and Gao, 2014). The study was performed to determine the mechanical properties of the material. Based on the study, the tensile stress-strain graph of 7075 aluminum alloy has been plotted. Figure 2.8.2 shows the stress-strain graph of 7075 aluminum alloy tensile test specimen.

The third study is on the effect of post weld heat treatment on microstructure, mechanical and corrosion behavior of high strength AA7075 aluminium alloy friction stir

welds (Kumar, Reddy and Rao, 2015). This study focused on few parameters to be looked at for AA7075 aluminium alloy material after post weld heat treatment was applied to the material. One of the parameters was the mechanical properties of the material. Tensile test has been done to get result on mechanical properties of the material. The data from tensile test was collected and plotted in the form of stress-strain graph to be analysed. Figure 2.8.3 shows the stress-strain graph for AA7075 aluminium alloy specimen after tensile test was done

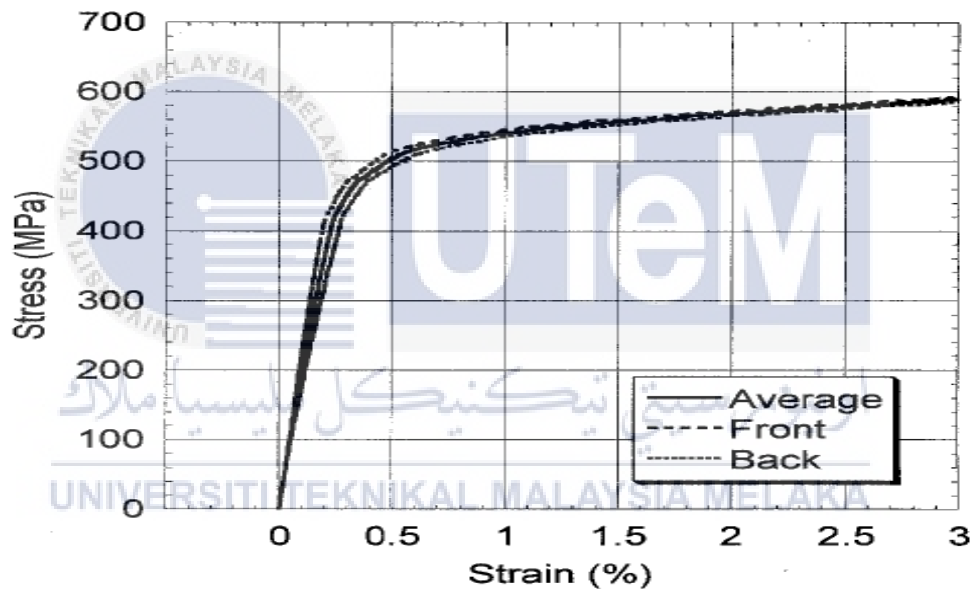


Figure 2.8.1: Stress-strain graph of well-aligned sample for tensile testing of micro sample

(Source: LaVan and Sharpe, 1999)

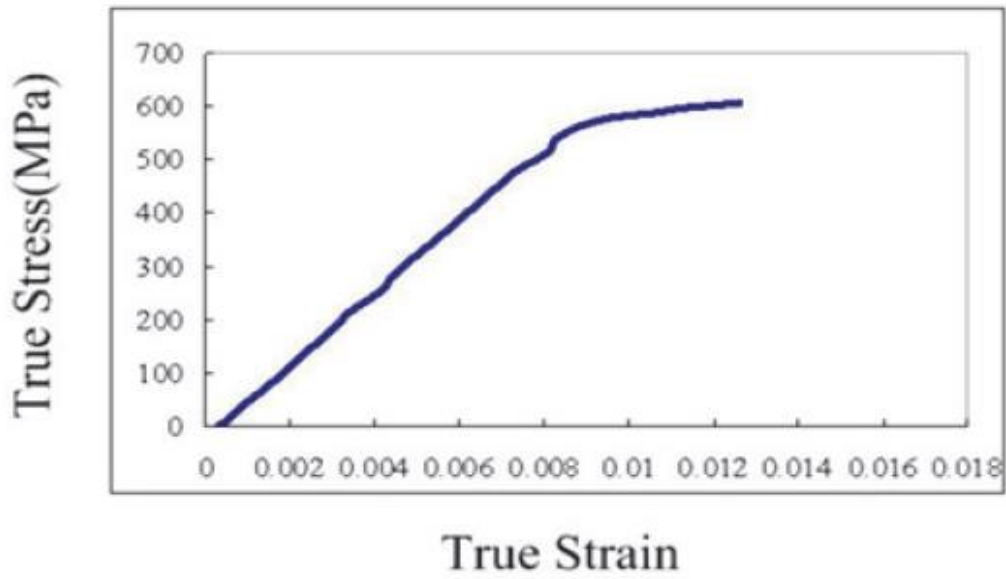


Figure 2.8.2: The stress-strain graph of 7075 aluminum alloy tensile test specimen

(Source: Chen, You and Gao, 2014)

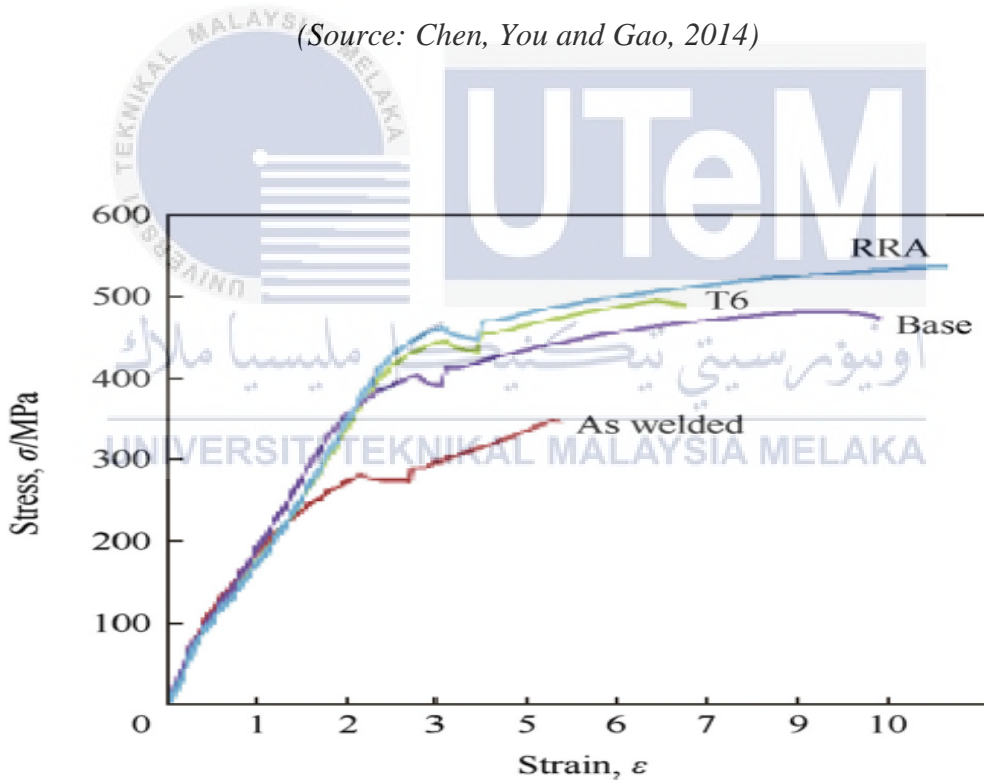


Figure 2.8.3: Stress-strain graph for AA7075 aluminum alloy specimen after tensile test

was done

(Source: Kumar, Reddy and Rao, 2015)

CHAPTER 3

METHODOLOGY

3.1 Introduction

In this chapter, workflow is decided as a guideline steps and procedure for this study. The workflow comprises stages of process. Beside literature studies and research, design and statistical analysis of data will be elaborated. The fabrication of specimens with different geometrical shape using 3D printing process and tensile test on specimens by using Shimadzu EZ Test (EZ-LX) test machine will be described.

3.2 Workflow Chart

Figure 3.2 presents the flowchart of methodology in this study. The flowchart listed the actions needed to be carried through out conducting this study. Firstly, literature studies are based from related articles, journals or any resources relevant to review on 3D printing, tensile test and geometrical shape effect on miniature specimen. Next, single struts are designed with and without geometrical shape using a computer-aided design (CAD) software which is Solidworks. In fabrication stage, the designed single struts are printed by using a 3D printer (CubePro machine) with the uses of ABS material. Then, the struts will undergo tensile test after the fabrication stage by using Shimadzu EZ Test (EZ-LX) machine. Analysis on mechanical characteristic results will be recorded and statistical analysis is used to further compare the mechanical characteristic. Lastly, report on the study will be written at the end of the study.

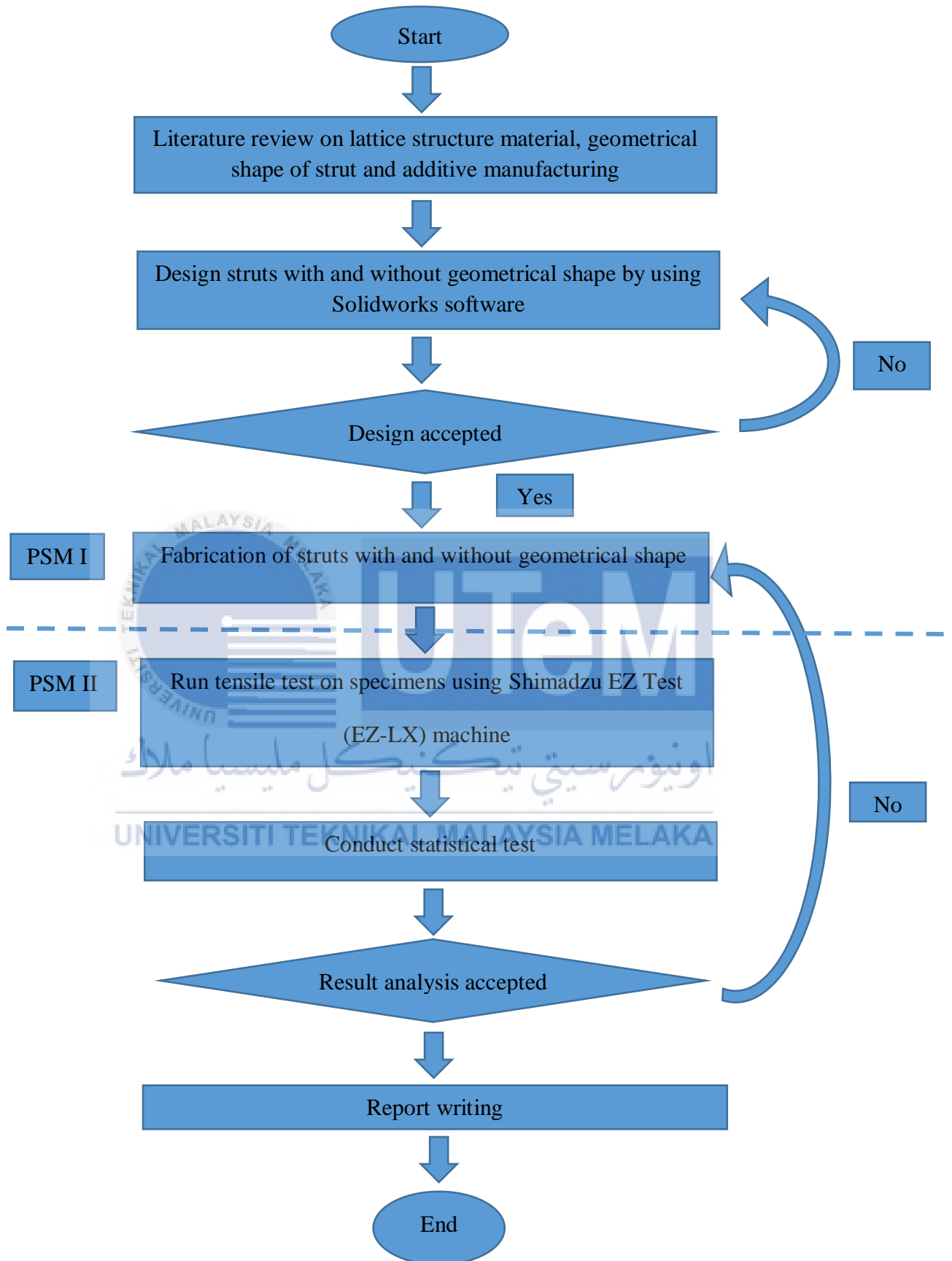


Figure 3.2: Flowchart of methodology

3.3 Design Stage

The design of specimen has been made by using the ratio which was referred to American Society of Testing for Material (ASTM) for standard tensile test specimen for metals which is E8/E8M-13a. Figure 3.3.1 shows the standard measurement for tensile test specimen for metal specimen.

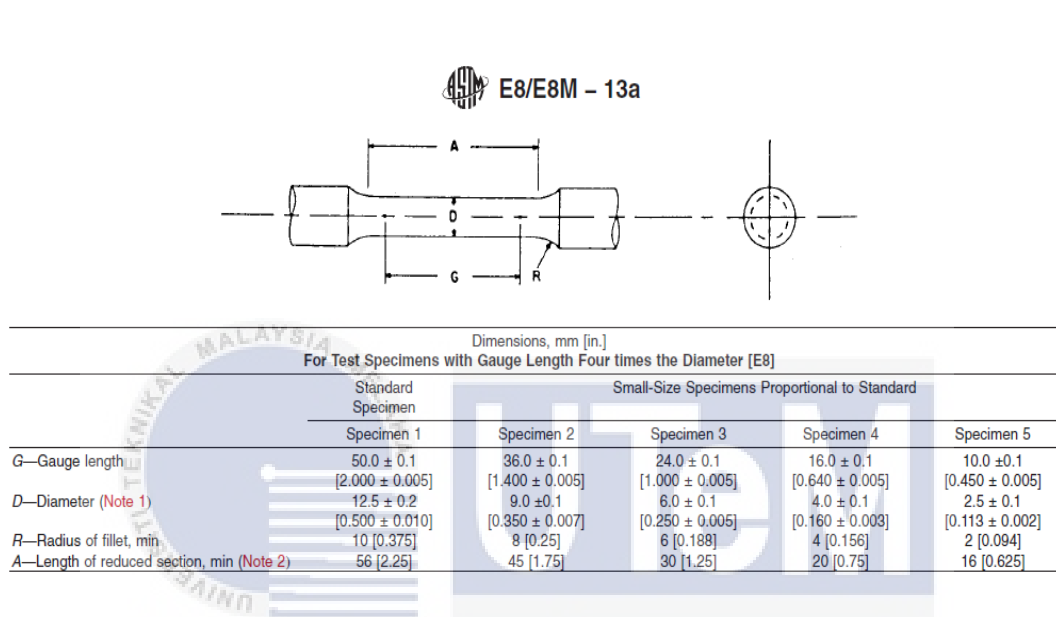


Figure 3.3.1: The standard measurement for tensile test specimen for metal

(Source: ASM Handbook, Volume 8: Mechanical Testing and Evaluation Online, 2000)

Table 3.3.1 shows details on single strut specimen for tensile test in this study. The design information is based on E8/E8M-13a as a guideline. The parameters of single strut are set for both with and without geometrical shape. There are forty five specimens to be fabricated to study and compare the elastic property of the single strut.

Table 3.3.1: Details on single strut specimen for tensile test

Type of strut	Single strut without geometrical shape, Cylinder			Single strut with geometrical shape, Dogbone					
				Dogbone1 (0.9mm fillet radius)			Dogbone2 (0.48mm fillet radius)		
Material	ABS			ABS			ABS		
Specimen ID	C			DB1			DB2		
	C_1	C_2	C_3	$DB1_1$	$DB1_2$	$DB1_3$	$DB2_1$	$DB2_2$	$DB2_3$
	C_4	C_5	C_6	$DB1_4$	$DB1_5$	$DB1_6$	$DB2_4$	$DB2_5$	$DB2_6$
	C_7	C_8	C_9	$DB1_7$	$DB1_8$	$DB1_9$	$DB2_7$	$DB2_8$	$DB2_9$
	C_{10}	C_{11}	C_{12}	$DB1_{10}$	$DB1_{11}$	$DB1_{12}$	$DB2_{10}$	$DB2_{11}$	$DB2_{12}$
	C_{13}	C_{14}	C_{15}	$DB1_{13}$	$DB1_{14}$	$DB1_{15}$	$DB2_{13}$	$DB2_{14}$	$DB2_{15}$
Specimen length (mm)	40								
Gauge length (mm)	8								
Built angle from horizontal (°)	35.26								
Lattice configuration reference to build single strut	BCC								

Solidworks is a CAD software that had been used to design and draw these 45 single struts. An example of a part drawing and a dimension drawing of single struts are shown in

Figure 3.3.2, 3.3.3, 3.3.4, 3.3.5, 3.3.6 and 3.3.7 respectively. The sidewalk support for each single strut is designed to ensure that strut can be printed successfully (Chen, 2008).

3D modelling of these single struts are selected after the design process is finished. Then, drawings are converted into “STL” (Standard Tessellation Language) file format in Solidworks software. After this, the STL file is transferred to the software of CubePro to create slices from the model of single struts for data preparation before producing the single struts.



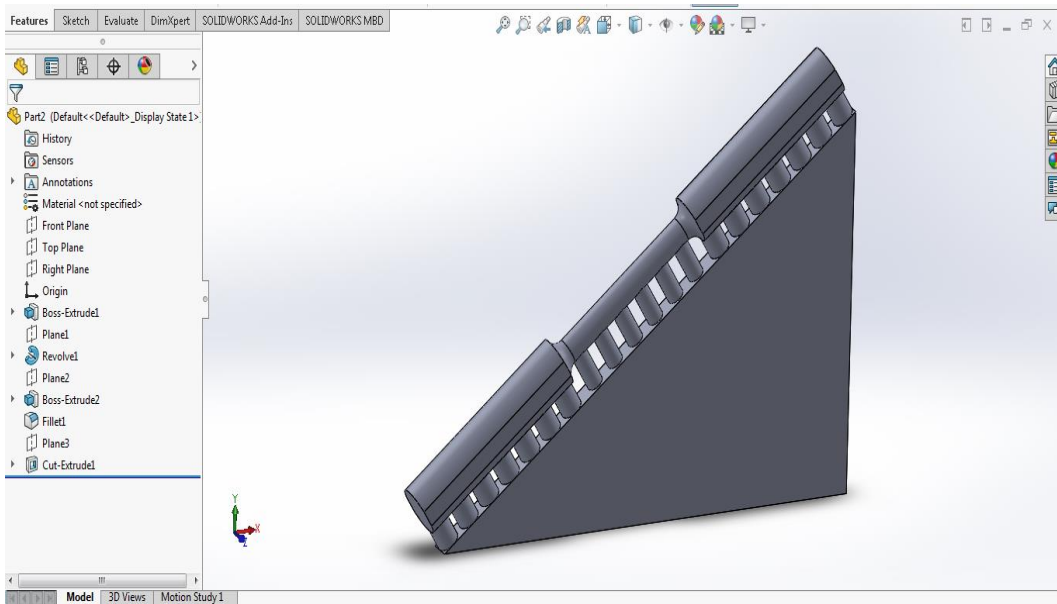


Figure 3.3.4: The part drawing of Dogbone1 (0.90 mm fillet radius) single struts using

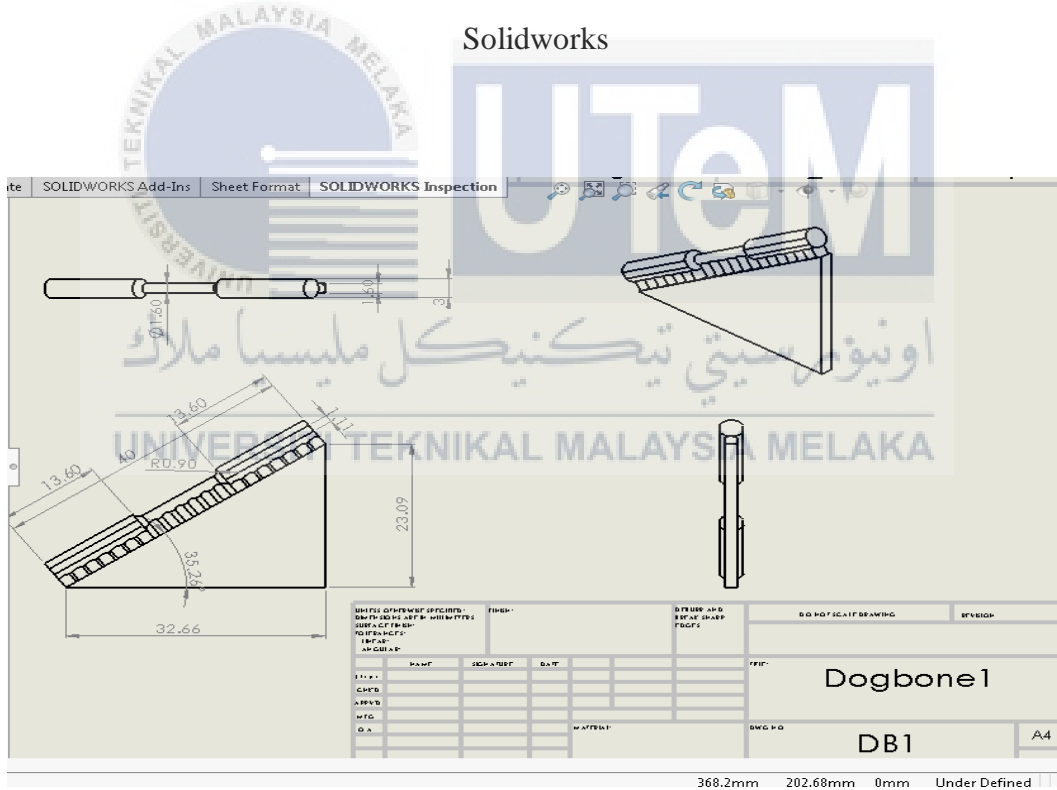


Figure 3.3.5: The part dimension drawing of Dogbone1 (0.90 mm fillet radius) single struts using Solidworks

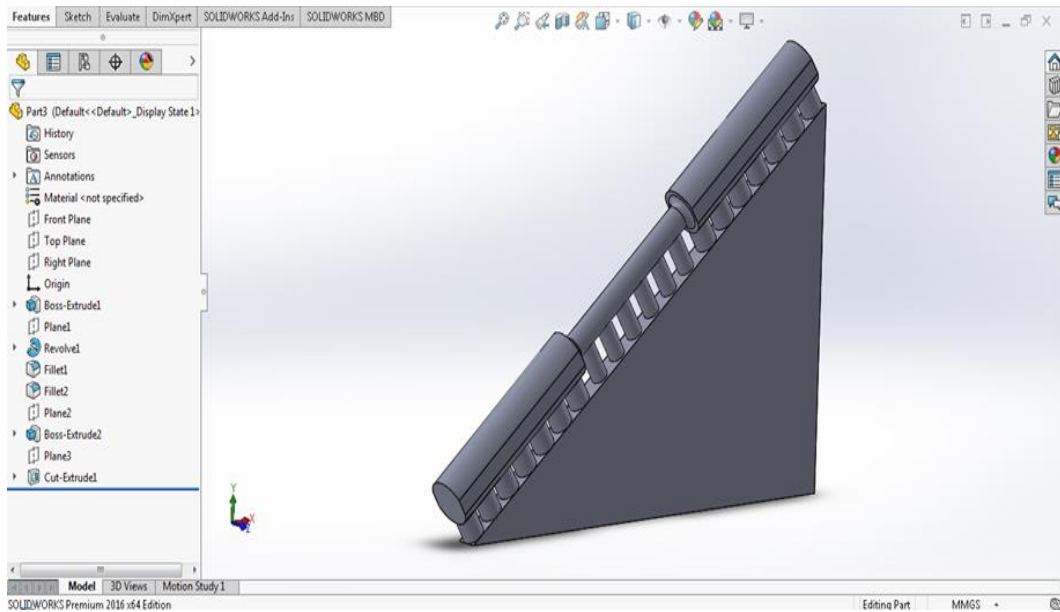


Figure 3.3.6: The part drawing of Dogbone2 (0.48 mm fillet radius) single struts using

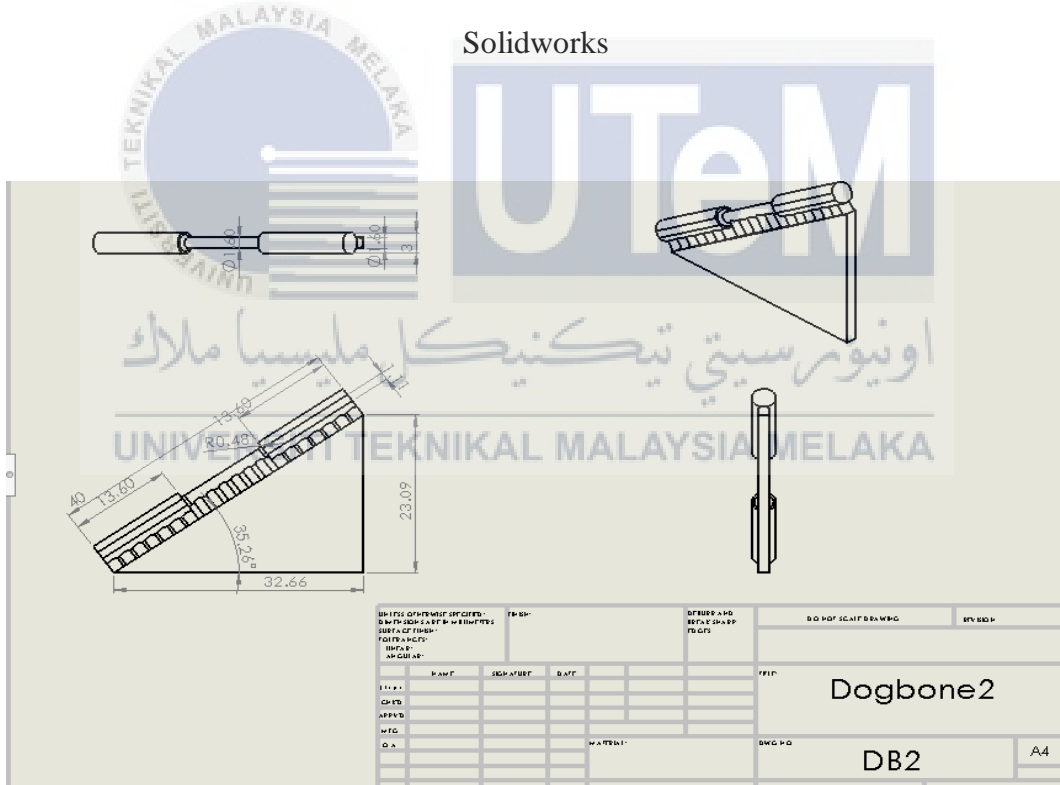


Figure 3.3.7: The part dimension drawing of Dogbone1 (0.48 mm fillet radius) single struts using Solidworks

3.4 Fabrication Stage

The STL file that has been saved from Solid works is opened in CubePro software to create slices of single struts model. Built setting is selected in CubePro software. This built setting is needed for the struts to be built layer by layer later on during 3D printing process. There are optional process parameters that can be chosen from the built settings in order to print the designed part. Figure 3.4.1 and 3.4.2 show the built settings and the descriptions from CubePro software. Figure 3.4.3 shows that the sidewalk support of single struts are generated itself by the software.



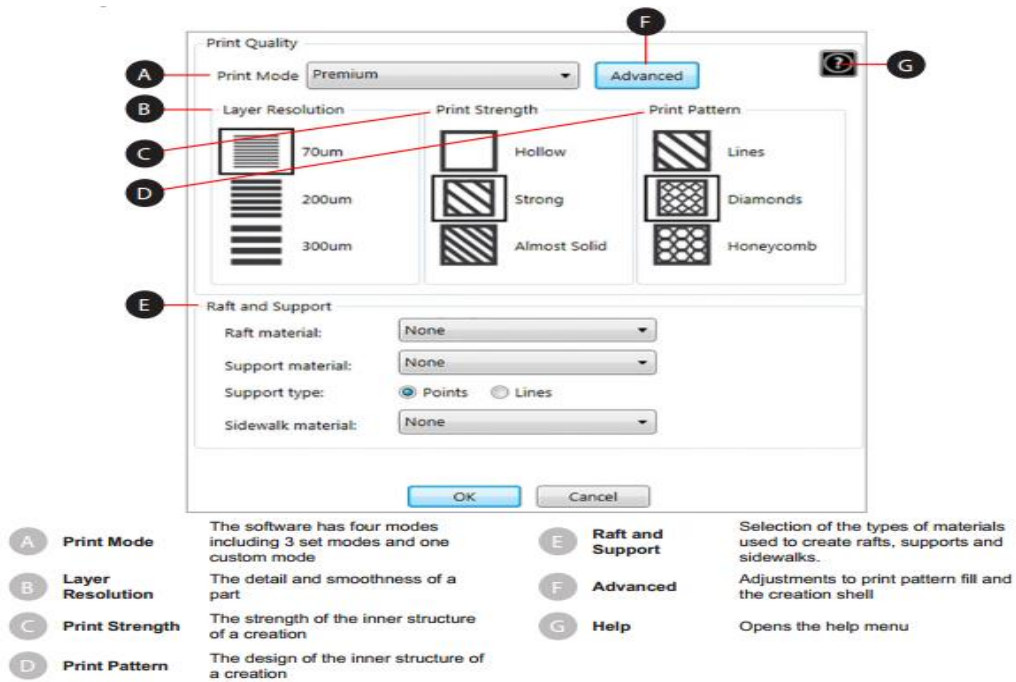


Figure 3.4.1: Build settings of CubePro software

(Source: 3D Systems Inc., 2015)

Print Mode	
Standard	<ul style="list-style-type: none"> Layer Resolution: 200um Print Strength: Strong Print Pattern: Diamonds
Premium	<ul style="list-style-type: none"> Layer Resolution: 70um Print Strength: Strong Print Pattern: Diamonds
Draft	<ul style="list-style-type: none"> Layer Resolution: 300um Print Strength: Strong Print Pattern: Lines
Custom	Custom allows the user to customize their print settings
Print Resolution	
0.070	<ul style="list-style-type: none"> Great mode for parts requiring smooth surfaces Layer lines are not very visible in these parts Good mode for artistic parts with a smooth flow Not the best mode for fine detail
0.200	<ul style="list-style-type: none"> Best mode for general printing and most compatible mode for a wide range of geometries Fine detail preservation for things like steeples, spires, sharp points, or thin walls
0.300	<ul style="list-style-type: none"> A fast mode with thicker layers Good for large parts with minimal detail
Print Strength	
Hollow	<ul style="list-style-type: none"> Fastest mode to produce a part Hollow has fewer outer surfaces and larger print pattern spacing Best for parts that will not be stressed
Strong	<ul style="list-style-type: none"> Medium amount of outer surfaces and smaller print pattern spacing Best for parts that will have minimal physical abuse
Almost Solid	<ul style="list-style-type: none"> The most surfaces and the tightest print pattern spacing The most robust part Best for parts that will be stressed
Print Pattern	
Lines	<ul style="list-style-type: none"> Fastest print fill pattern Minimal cross bracing
Diamonds	<ul style="list-style-type: none"> Strong print pattern with 2-direction cross bracing
Honeycomb	<ul style="list-style-type: none"> Strong print pattern with 3-direction cross bracing

Figure 3.4.2: Descriptions on the build settings

(Source: 3D Systems Inc., 2015)

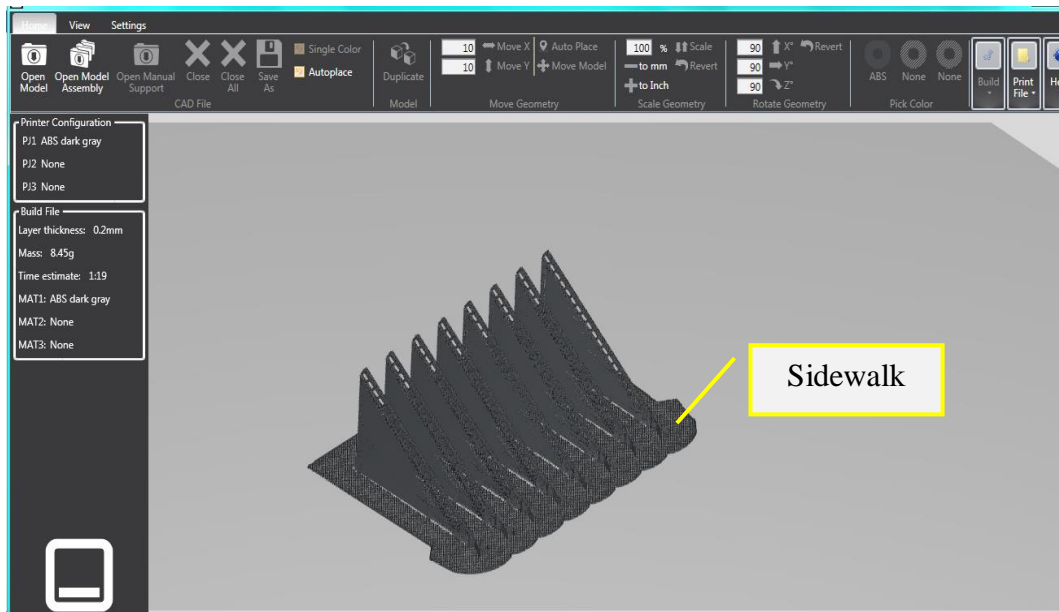


Figure 3.4.3: Single struts with slices in CubePro software

In order for single struts in this study to be produced at its best form, the most suitable parameters for single struts specimen in this study are chosen. The parameters are chosen after few fabrication trials of different setting on the parameters. For this study, the parameters selected for both dogbone and cylinder single strut are shown in Figure 3.4.4. This is similar to that done in previous studies (Chen, 2018; Wahi, 2018).

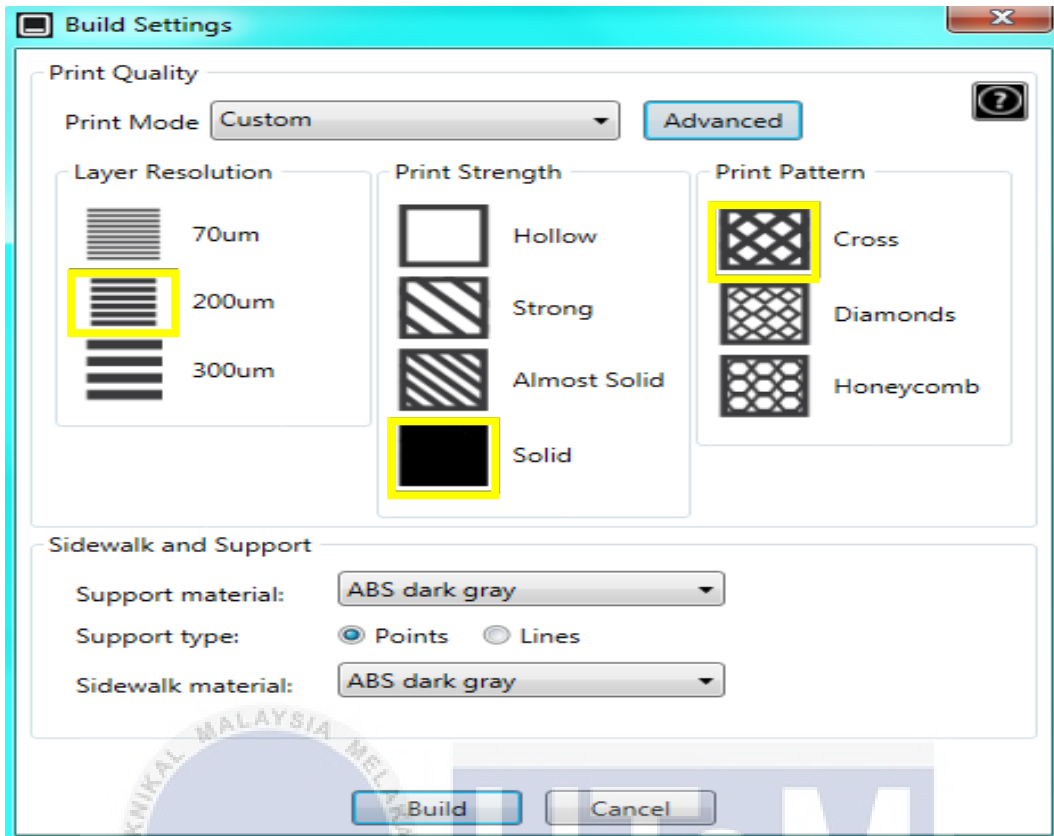


Figure 3.4.4: Parameters selected for both dogbone and cylinder single strut

3.5 Tensile test

Tensile test is needed to be conducted to analyse the strength and the mechanical properties of single strut specimen. Figure 3.5.1 shows the Shimadzu EZ Test (EZ-LX) test machine used to conduct tensile test. ASTM D638 for tensile test standard is referred in this research as a guideline (Raney et al., 2017). Shimadzu EZ Test (EZ-LX) can exert up to 1kN load capacity and it is controlled by Trapezium X software window as shown in Figure 3.5.2. In this study, the tensile load cell and tensile speed for dogbone and cylinder shape single strut are the same. The load cell used for the tensile test specimen is 1 kN and the speed of tensile test is at 0.1 mm per minute. The raw data of tensile test are including force, time and stroke recorded from the Trapezium X software. This data will be used to produce stress versus strain graph. Hypothesis test is used to analyze the data.



Figure 3.5.1: Shimadzu EZ Test (EZ-LX) test machine



Figure 3.5.2: Trapezium X software window

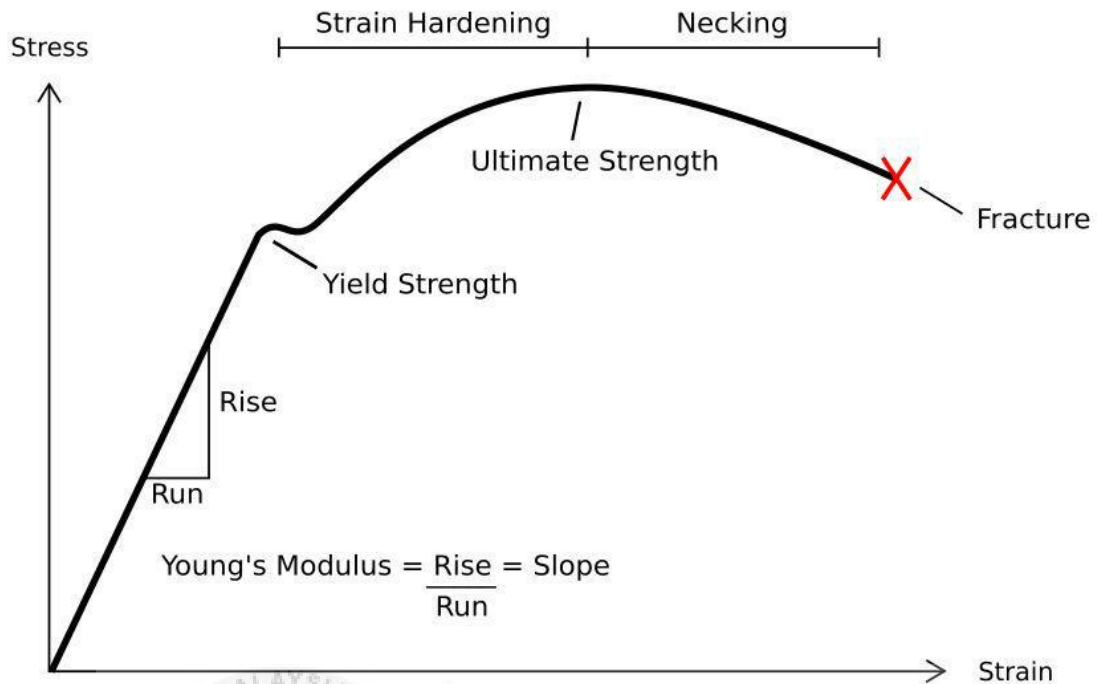


Figure 3.5.3: Graph to find Young's modulus

(Source: *Solid Mechanics*, 2010)

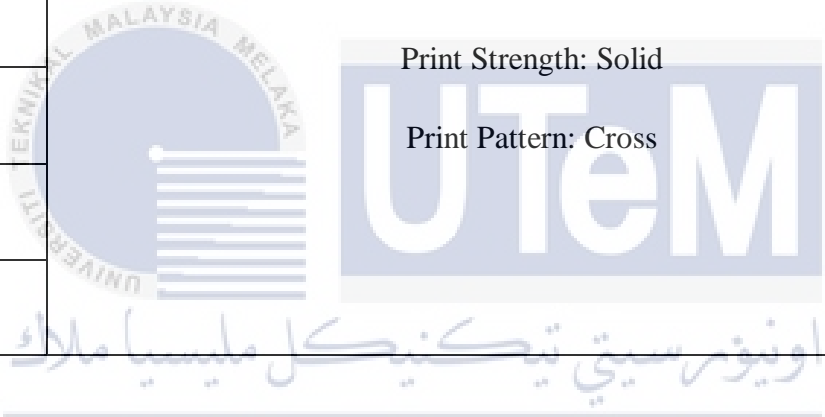
Figure 3.5.3 shows the method to find Young's modulus. A raw data from Trapezium X software are used to plot tensile stress versus tensile strain graph. To determine Young's modulus, a trend line for obtained stress strain graph will be plotted. The gradient under the graph for the elastic region will be determined. The gradient is determined by the rise over run.

3.6 Hypothesis Test

Comparative method will be used to analyse the effect of geometrical shape towards the elastic property. Dogbone and cylinder single strut will be compared in this method. There are five batches of single strut specimen that are being fabricated for both cases. First case would be single strut specimen with geometrical shape while the second case would be

single strut specimen without geometrical shape. The process parameter used in CubePro 3D printer is shown in Table 3.6.1.

Table 3.6.1: Process parameters selected in CubePro 3D printer

Batch	With geometrical shape (Case 1)		Without geometrical shape (Case 2)
	Dogbone1 (0.9mm fillet)	Dogbone2 (0.48mm fillet)	Cylinder
1			
2			
3			
4			
5			

There are 45 struts that represent single strut specimen with and without geometrical shape. These struts are printed with same properties; 200 μm layer solution, solid printed strength and cross printed pattern, but the strength of these two different types of strut is expected to be different. Hypothesis test (Kuang, 2007) will be carried out to ascertain if geometrical shape does effect on strength of specimen. Hypothesis test will include both F-test and t-test to be carried out as shown in Figure 3.6.1.

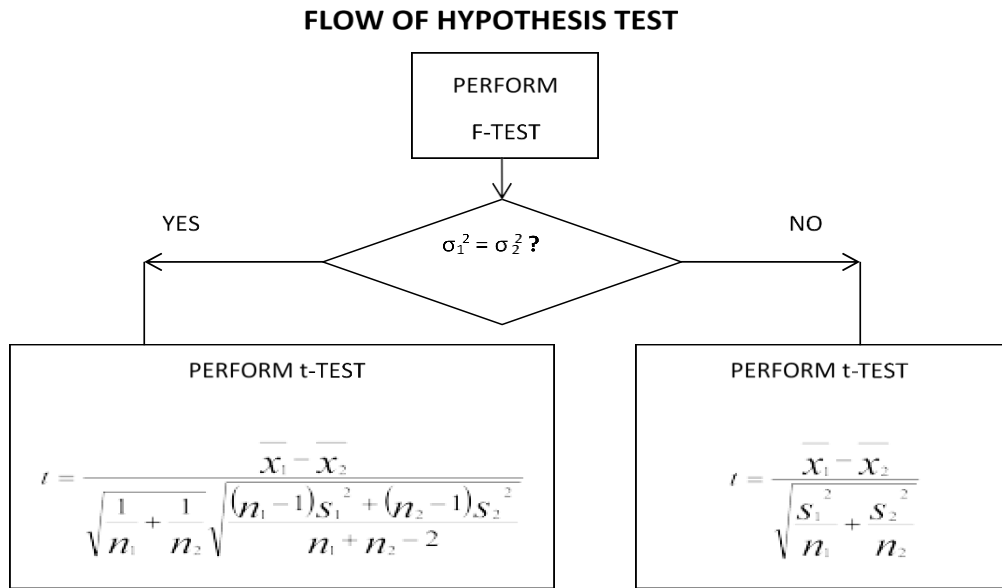


Figure 3.6.1: Flow of hypothesis test.

(Source: Kuang, 2007)

3.6.1 Testing of Variances (F-Test)

F-test is the first test that needs to be carried out as the acceptance region in the F-test will show either the theory made is matched with the test or not. The steps for hypothesis test are described in the followings.

Step 1:

Hypothesis theory. In this step, H_0 and H_1 need to be determined.

$H_0 =$ Elastic strength of single strut specimen with geometrical shape is the same with elastic strength of single strut specimen without geometrical shape

$H_1 =$ Elastic strength of of single strut specimen with geometrical shape is different with elastic strength of single strut specimen without geometrical shape

Where,

$H_0: \sigma_1^2 = \sigma_2^2$

$H_1: \sigma_1^2 \neq \sigma_2^2$

$\sigma =$ Variences

Step 2:

The α risk (significant level). In this step, there are two α risks.

5 % : If we are fairly ready to change our minds.

1 % : If we are hard to convince.

The α risk choose is 0.005 (5%).

Step 3:

The difference of variances, test statistic need to be determined.

$$F = \frac{S_1^2}{S_2^2} \tag{3.1}$$

Where, (3.2)

$$S = \sqrt{\frac{\sum(X_i - X)^2}{n-1}}$$

$$\begin{aligned}
 \text{F distributed, } DF_1 &= n_1 - 1 \\
 &= 15 - 1 \\
 &= 14
 \end{aligned}$$

$$\begin{aligned}
 \text{Degree of freedom, } DF_2 &= n_2 - 1 \\
 &= 15 - 1 \\
 &= 14
 \end{aligned}$$

Where,

S = Standard deviation

x = mean

n = number of sets

Step 4:

Determine either one or two tail test.

Comparing variance:

$$\begin{aligned}
 H_0 : & \quad \sigma_1^2 = \sigma_2^2 \\
 H_1 : & \quad \left. \begin{array}{l} \sigma_1^2 > \sigma_2^2 \\ \sigma_1^2 < \sigma_2^2 \end{array} \right\} \text{one tail} \\
 & \quad \left. \begin{array}{l} \sigma_1^2 < \sigma_2^2 \\ \sigma_1^2 \neq \sigma_2^2 \end{array} \right\} \text{two tails}
 \end{aligned}$$

Since $H_1 : \sigma_1^2 \neq \sigma_2^2$, this is two tails test.

Step 5:

The acceptance region for H_1 need to be determined. The range of values of the test statistic which result in decision to accept the H_1 hypothesis.

Step 6:

After the samples of observations are obtained, the test statistic needs to be computed.

Step 7:

The computed test statistic value will be compared to the acceptance region to make a decision either α risk is accepted or not.

Step 8:

An engineering conclusion will be drawn.

3.6.2 Comparison of Means (T-Test)

The T-test is differ from F-test as T-test is using means while F-test is using variances. The previous study result from F-test will be conclude and used to satisfy the assumption on equal variance of populations. After F-test is done, T-test will be carried out. The steps for T-test are described in the followings.

Step 1:

State the H_0 and H_1 in term of means.

$H_0 =$ Elastic strength of single strut specimen with geometrical shape is the same with elastic strength of single strut specimen without geometrical shape ($\mu_1 = \mu_2$).

Elastic strength of of single strut specimen with geometrical shape is lower with elastic strength of single strut specimen without geometrical shape ($\mu_1 < \mu_2$).

Where μ is a mean

Step 2:

Choose α risk. The α risk choose is 0.05 (5%)

Where α risk is a significant level

Step 3:

The difference of means on mean for elastic strength of single strut specimen with geometrical shape is higher than that of elastic strength of single strut specimen without geometrical shape. The F-test result will be used to determine which formula needs to be used to calculate the test statistic.

If $\sigma_1^2 = \sigma_2^2$ the formula for test statistic is

$$t = \frac{\bar{x}_1 - \bar{x}_2}{\sqrt{\frac{1}{n_1} + \frac{1}{n_2}} \sqrt{\frac{(n_1-1)s_1^2 + (n_2-1)s_2^2}{n_1 + n_2 - 2}}} \quad (3.3)$$

If $\sigma_1^2 \neq \sigma_2^2$, the formula for test statistic is

$$t = \frac{\bar{x}_1 - \bar{x}_2}{\sqrt{\frac{s_1^2}{n_1} + \frac{s_2^2}{n_2}}} \quad (3.4)$$

Where DF = $n_1 + n_2 - 2$

$$= 15 + 15 - 2$$

$$= 28$$

t = test statistics

x = Means

S = standard deviation

DF = Degree of Freedom

n = Number of sets

Step 4 :

Determine either H_1 is one tail or two tail test.

Comparing means:

$H_0 :$ $\mu_1 > \mu_2$

$H_1 :$ $\mu_1 > \mu_2$: one tail

$\mu_1 < \mu_2$
: two tails

$\mu_1 \neq \mu_2$

Since $H_1 : \mu_1 < \mu_2$, this is one tail test.

Step 5:

The acceptance region for H_1 needs to be determined. The range of values of the test statistic which result in decision to accept the H_1 hypothesis.

Step 6:

After the samples of observations are obtained, the test statistic needs to be computed.

Step 7:

The computed test statistic value will be compared to the acceptance region to make a decision either α risk is accepted or not.

Step 8:

An engineering conclusion will be drawn.

CHAPTER 4

RESULT AND DISCUSSION

4.1 Introduction

The acquired results will be discussed clearly in this chapter. The conclusion on Young's Modulus will be made between single strut specimens with and without geometrical shape. These results are obtained after few stages are completed which include design stage, tensile test stage and analysis stage.

4.2 Design stage

Based on the result in PSM I, the results are based on two types of specimen which are single strut specimens with and without geometrical shape. In PSM II the research continues by adding another specimen which is single strut specimen with geometrical shape of 0.48 mm radius fillet to see the significance of geometrical shape on mechanical property of single strut specimen. The radius of 0.48mm fillet for the design is referred from the stress-concentration factor, k_t for a filleted shaft in tension as shown in Figure 4.2.1. Figure 4.2.2, Figure 4.2.3 and Figure 4.2.4 show the dimension designed for single strut specimens with and without geometrical shape respectively.

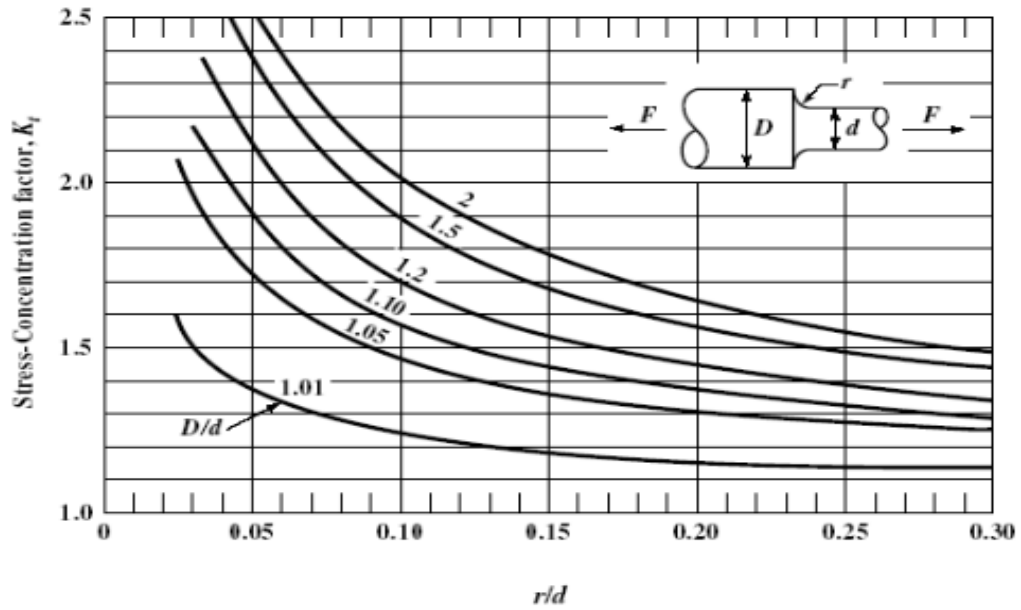


Figure 4.2.1: Stress-concentration factor, k_t for a filleted shaft in tension

(Source: Peterson's Stress Concentration Factors, 3rd Edition, 2008)

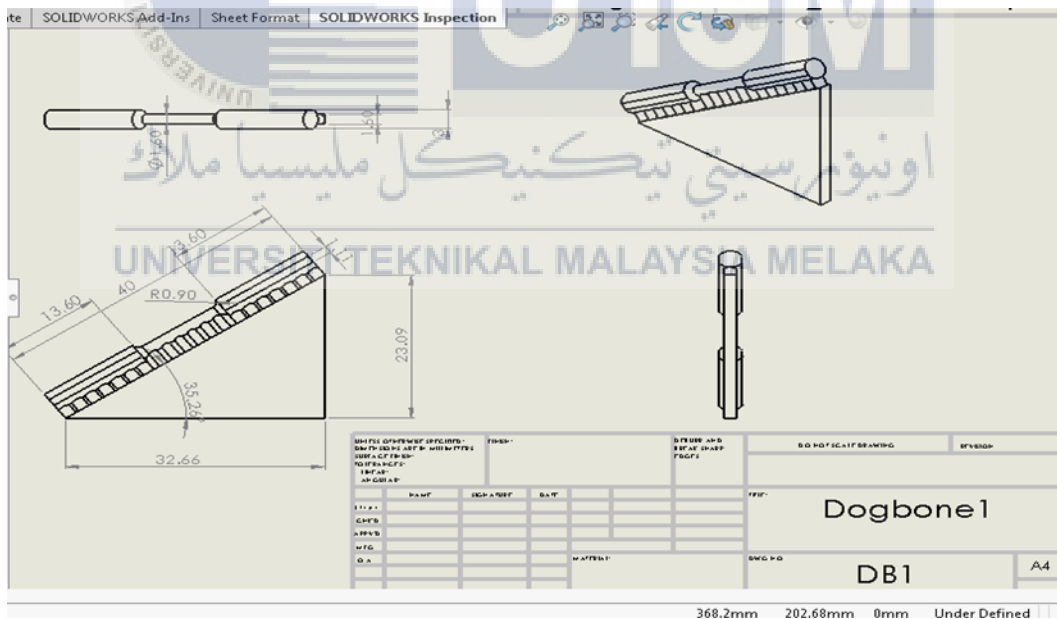


Figure 4.2.2: Design with dimension for single strut specimen with geometrical shape, Dogbone1 (0.90 mm fillet radius)

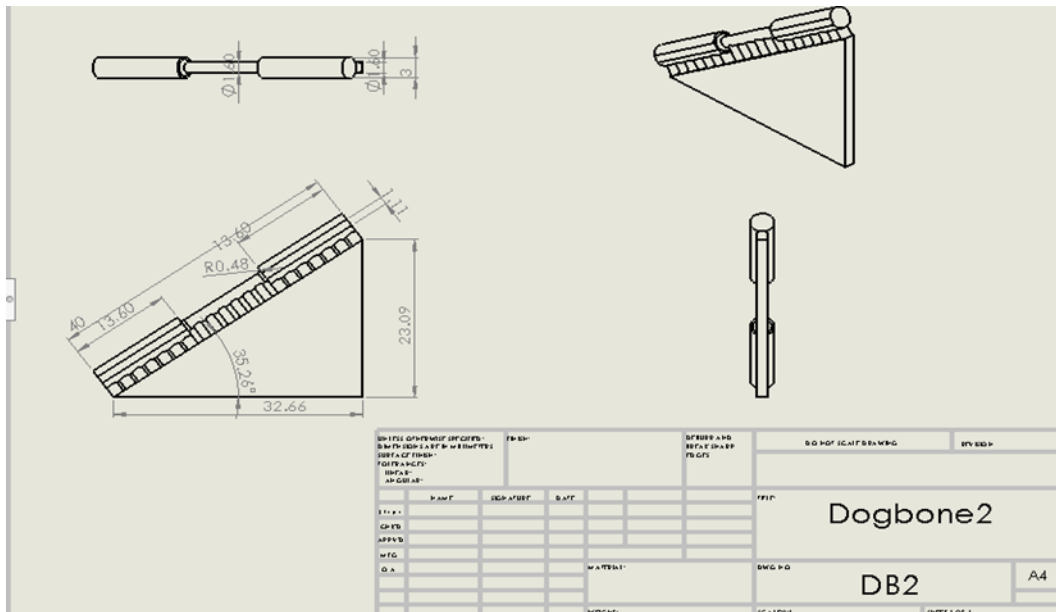


Figure 4.2.3: Design with dimension for single strut specimen with geometrical shape, Dogbone2 (0.48 mm fillet radius)

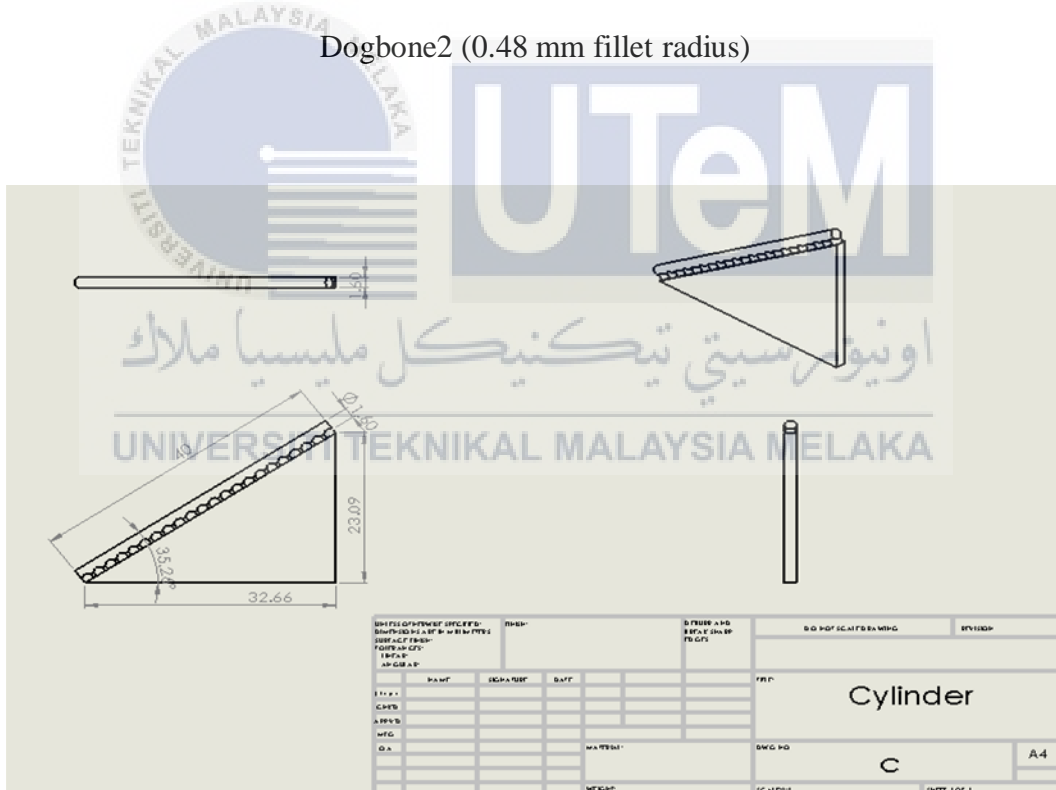


Figure 4.2.4: Design with dimension for single strut specimen without geometrical shape, Cylinder

4.3 Tensile test

The tensile test results from Trapezium X software are transferred into excel graph to determine the Young's modulus of single strut specimen. Figure 4.3.1, Figure 4.3.2 and Figure 4.3.3 show the tensile stress against tensile strain graph for cylinder and dogbone single strut respectively. The Young's modulus values calculated for cylinder and dogbone single struts are shown in Table 4.3.1.

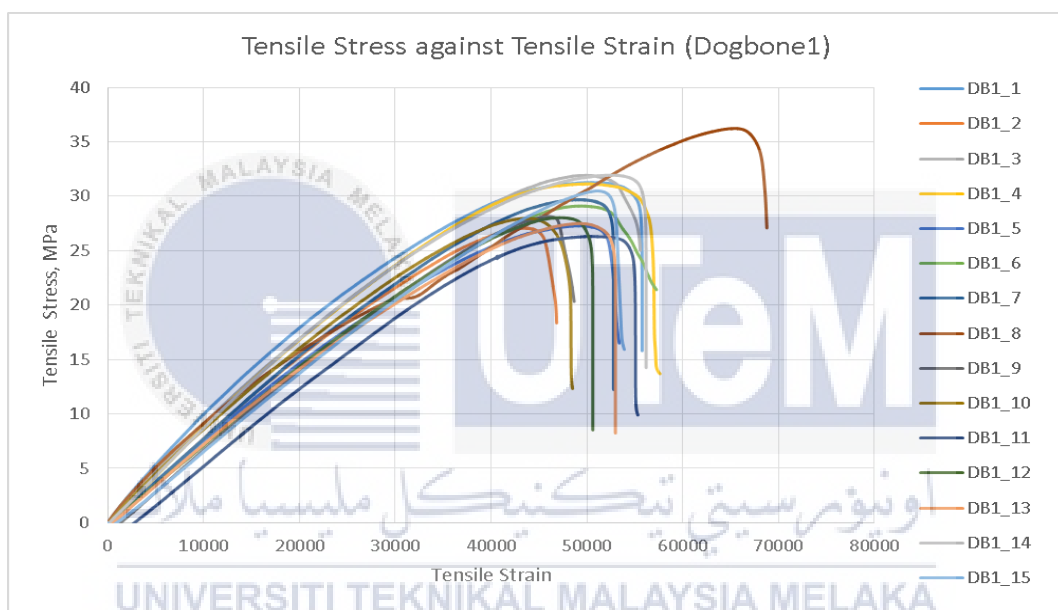


Figure 4.3.1: Stress-strain graph of dogbone single strut specimen for 0.9mm fillet radius (single strut specimen with geometrical shape), Dogbone1

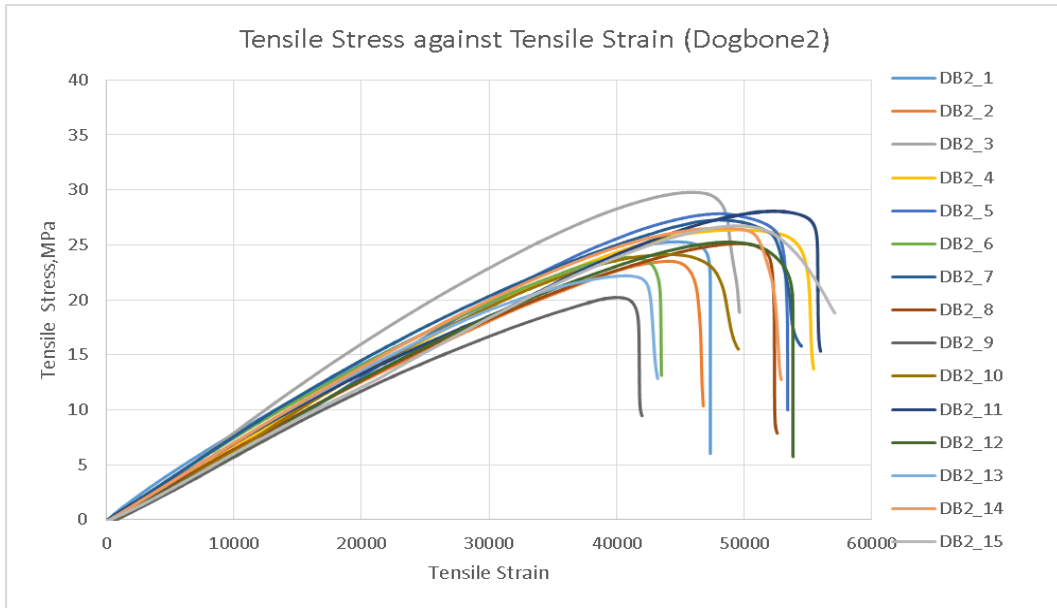


Figure 4.3.2: Stress-strain graph of dogbone single strut specimen for 0.48mm fillet radius (single strut specimen with geometrical shape), Dogbone2

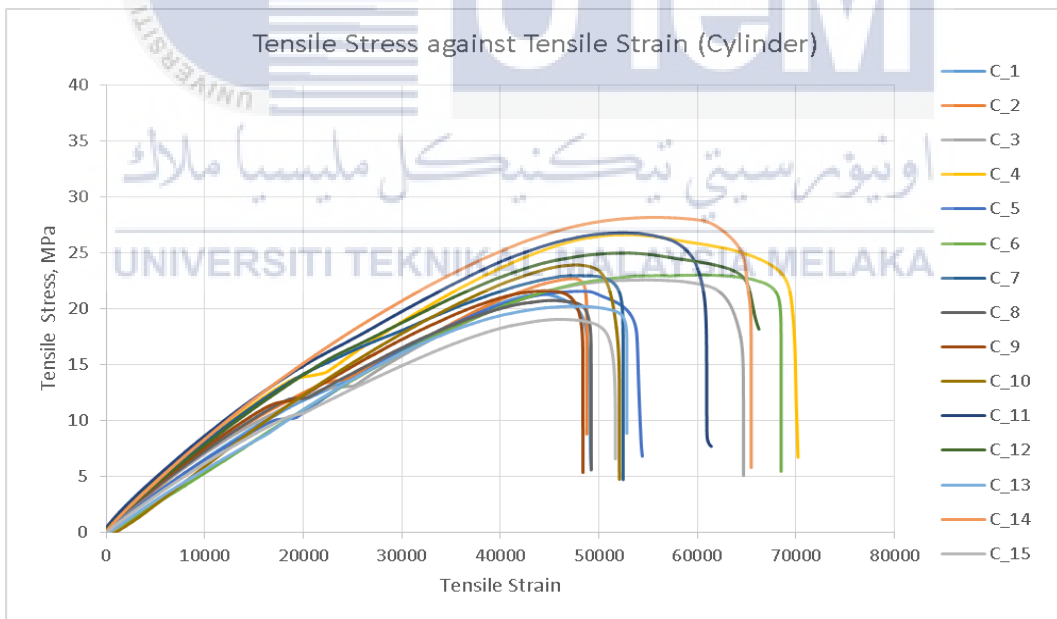


Figure 4.3.3 : Stress-strain graph of cylinder single strut specimen (single strut specimen without geometrical shape)

Table 4.3.1: Young's modulus values for cylinder and dogbone single struts

Number of specimen	Young's modulus, E (MPa). $E = \frac{y_2 - y_1}{x_2 - x_1}$		
	Cylinder (single strut specimen without geometrical shape)	Dogbone (single strut specimen with geometrical shape) with 0.9mm radius fillet	Dogbone (single strut specimen with geometrical shape) with 0.48mm radius fillet
1	292.2374	422.5817	171.123
2	332.2949	377.2102	296.6625
3	289.3913	437.3576	372.9604
4	369.1801	408.9457	214.2422
5	297.8129	364.1882	330.9204
6	257.7873	339.7028	331.0916
7	337.9092	368.3807	356.7447
8	328.8798	342.6124	308.1862
9	382.7751	332.8133	280.5787
10	296.2049	381.7477	301.6023
11	364.6031	312.3475	315.7895
12	325.9762	349.2179	300.9404
13	306.8073	333.6809	333.1598
14	371.2297	384.3844	334.0292
15	278.503	327.9809	283.8137

4.4 Analysis

Young's modulus values have been determined for each specimen for both single strut with and without geometrical shape and are shown in Table 4.3.1. Hypothesis test has been carried out to analyse the data.

4.4.1 Young's modulus for Cylinder and Dogbone1

Testing of variances (F-TEST):

Hypothesis theory needs to be determined.

$H_0 =$ Young's modulus of single strut specimen with geometrical shape is the same with single strut specimen without geometrical shape

$H_1 =$ Young Modulus of single strut specimen with geometrical shape is the different with single strut specimen without geometrical shape

After that choose α risk (significant level).

5%: if we are fairly ready to change our minds.

The risk is chosen as 0.05 (5%).

Single strut specimen without geometrical shape (Cylinder), S_1

292.237, 332.295, 289.391, 369.180, 297.813
257.787, 337.909, 328.880, 382.775, 296.205
364.603, 325.976, 306.807, 371.230, 278.503

Calculate mean, X'

$$\begin{aligned} X' &= \frac{292.237 + 332.295 + 289.391 + 369.180 + 297.813 + 257.787 + 337.909 + 328.880 + 382.775 + 296.205 + 364.603 + 325.976 + 306.807 + 371.230 + 278.503}{15} \\ &= \frac{4831.591}{15} \\ &= 322.106 \end{aligned}$$

Table 4.4.1.1: Summation on means of Young's modulus for single strut specimen without geometrical shape (Cylinder) F-TEST, S_1

X_i	$X_i - X'$	$(X_i - X')^2$
292.237	-29.869	892.157
332.295	10.189	103.816
289.391	32.715	1070.271
369.180	47.074	2215.961
297.813	-24.293	590.150
257.787	-64.319	4136.934
337.909	15.803	249.735
328.880	6.774	45.887
382.775	60.669	3680.728
296.205	-25.901	670.862
364.603	42.497	1805.995
325.976	3.87	14.977
306.807	-15.299	234.059
371.230	49.124	2413.167
278.503	-43.603	1901.222

From Table 4.4.1.1,

$$\begin{aligned}
 \sum (X_i - X') &= 892.157 + 103.816 + 1070.271 + 2215.961 + 590.150 + 4136.934 \\
 &\quad + 249.735 + 45.887 + 3680.728 + 670.862 + 1805.995 + 14.977 \\
 &\quad + 234.059 + 2413.167 + 1901.222 \\
 &= 20025.921
 \end{aligned}$$

$$S_1 = \sqrt{\frac{20025.921}{14}}$$

$$= 37.821$$

$$S_1^2 = (37.821)^2$$

$$= 1430.428$$

Single strut specimen with geometrical shape (Dogbone1), S_2

422.582, 377.210, 437.358, 408.946, 364.188

339.703, 368.381, 342.612, 332.813, 381.748

312.347, 349.218, 333.681, 384.384, 327.981

Calculate mean, \bar{X}

$$\bar{X} = \frac{422.582 + 377.210 + 437.358 + 408.946 + 364.188 + 339.703 + 368.381 + 342.612 + 332.813 + 381.748 + 312.347 + 349.218 + 333.681 + 384.384 + 327.981}{15}$$

$$= \frac{5483.152}{15}$$

$$= 365.543$$

Table 4.4.1.2: Summation on means of Young's modulus for single strut specimen with geometrical shape (Dogbone1) F-TEST, S_2

X_i	$X_i - \bar{X}$	$(X_i - \bar{X})^2$
422.582	57.039	3253.448
377.210	11.667	136.119
437.358	71.815	5157.394
408.946	43.403	1883.820
364.188	-1.355	1.836
339.703	-25.84	667.706
368.381	2.838	8.054
342.612	-22.931	525.831
332.813	-32.73	1071.253
381.748	16.205	262.602
312.347	-53.196	2829.814
349.218	-16.325	266.506
333.681	-31.862	1015.187
384.384	18.841	354.983
327.981	-37.562	1410.904

From Table 4.4.1.2,

$$\begin{aligned} \sum (X_i - \bar{X})^2 &= 3253.448 + 136.119 + 5157.394 + 1883.820 + 1.836 + 667.706 \\ &\quad + 8.054 + 525.831 + 1071.253 + 262.602 + 2829.814 \\ &\quad + 266.506 + 1015.187 + 354.983 + 1410.904 \end{aligned}$$

$$= 18845.457$$

$$S_2 = \sqrt{\frac{18845.457}{14}}$$

$$= 36.689$$

$$S_2^2 = (36.689)^2$$

$$= 1346.083$$

F Distributed,

Degree of freedom,

$$\begin{aligned} DF_1 &= n_1 - 1 \\ &= 15 - 1 \\ &= 14 \end{aligned}$$



Degree of freedom,

$$\begin{aligned} DF_2 &= n_2 - 1 \\ &= 15 - 1 \\ &= 14 \end{aligned}$$

Based on statement $H_1, \sigma_1 \neq \sigma_2$. Hence, the test is two tail test.

Acceptance region,

$$F > F_{0.975,14,14} = 2.9786$$

$$F < F_{0.025,14,14} = \frac{1}{2.9786}$$

$$\begin{aligned}
 &= 0.3357 \\
 F_{cal} &= \frac{1430.428}{1346.083} \\
 &= 1.0627
 \end{aligned}$$

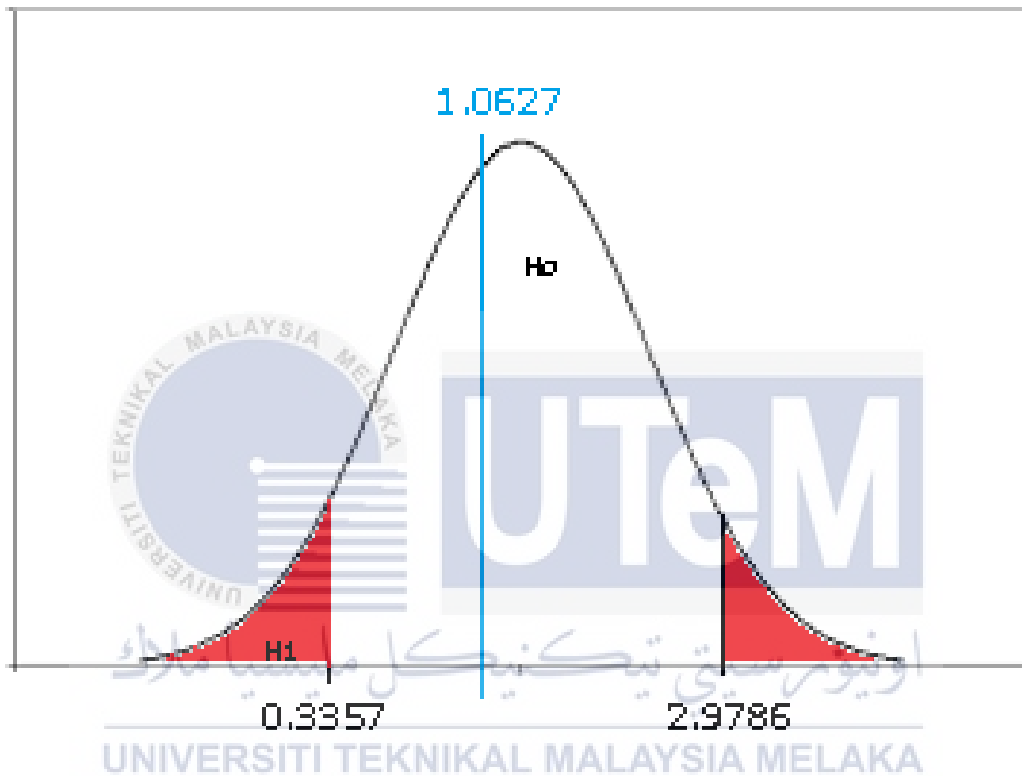


Figure 4.4.1.1: Bell graph for variance at 5% significant level for Cylinder and Dogbone1
(0.9mm radius fillet)

From Figure 4.4.1.1, engineering conclusion;

Single strut with geometrical shape shows no significant different in variance at 5% significant level.

Comparison of means (t-TEST)

From F-TEST result, $\sigma_1 = \sigma_2$. Therefore formula used for t-TEST is

$$t = \frac{\tilde{x}_1 - \tilde{x}_2}{\sqrt{\frac{1}{n_1} + \frac{1}{n_2}} \sqrt{\frac{(n_1 - 1)s_1^2 + (n_2 - 1)s_2^2}{n_1 + n_2 - 2}}}$$

Where,

$$X'_1 = 322.106$$

$$X'_2 = 365.543$$

$$S_1^2 = 1430.428$$

$$S_2^2 = 1346.083$$

$$N_1 = 15$$

$$N_2 = 15$$

$H_0 =$ Young Modulus of single strut specimen with geometrical shape is the same with single strut specimen without geometrical shape ($\mu_1 = \mu_2$)

$H_1 =$ Young Modulus of single strut specimen with geometrical shape is the different with single strut specimen without geometrical shape ($\mu_1 < \mu_2$)

$$h_0 : \mu_1 - \mu_2 \geq 0$$

$$h_1 : \mu_1 - \mu_2 < 0$$

Since $h_1 : \mu_1 - \mu_2 < 0$, this is one tail test

$$\begin{aligned}
 \text{Where DF} &= n_1 + n_2 - 2 \\
 &= 15 + 15 - 2 \\
 &= 28
 \end{aligned}$$

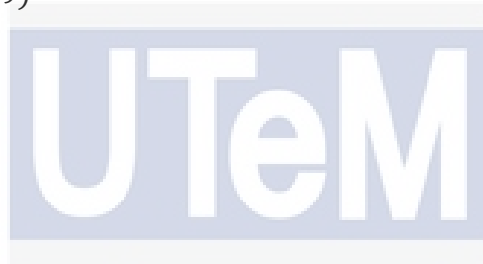
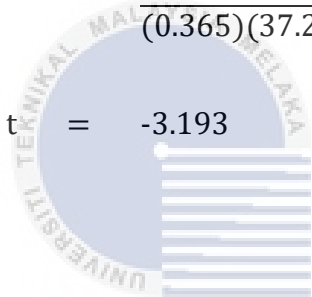
Acceptance region, H_1

$$t > t_{0.95,28} = 1.701$$

$$t = \frac{322.106 - 365.543}{\sqrt{\frac{1}{15} + \frac{1}{15}} \sqrt{\frac{(15-1)(1430.428) + (15-1)(1346.083)}{15+15-2}}}$$

$$t = \frac{-43.437}{(0.365)(37.259)}$$

$$t = -3.193$$



اونيورسيتي تيكنيكل مليسيا ملاك

UNIVERSITI TEKNIKAL MALAYSIA MELAKA

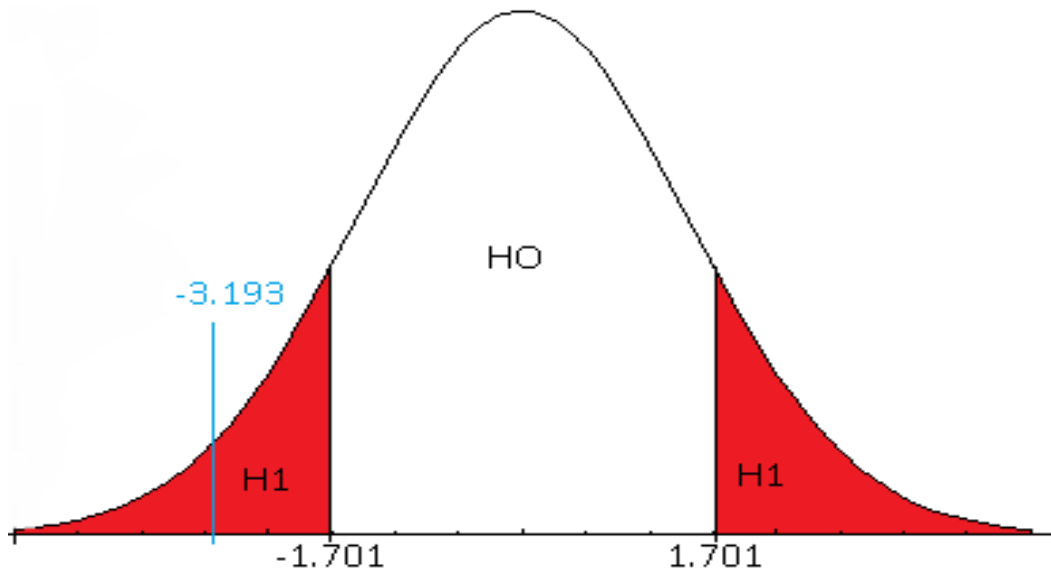
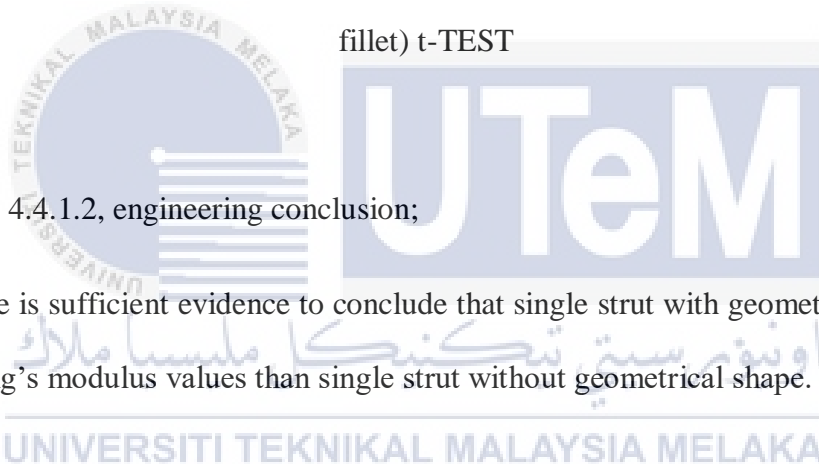


Figure 4.4.1.2: Bell graph for Young's modulus of Cylinder and Dogbone1 (0.9mm radius



fillet) t-TEST

From Figure 4.4.1.2, engineering conclusion;

There is sufficient evidence to conclude that single strut with geometrical shape has higher Young's modulus values than single strut without geometrical shape.

4.4.2 Young's modulus for Cylinder and Dogbone2

Testing of variances (F-TEST):

Hypothesis theory needs to be determined.

$H_0 =$ *Young's modulus of single strut specimen with geometrical shape is the same with single strut specimen without geometrical shape*

$H_1 =$ Young Modulus of single strut specimen with geometrical shape is the different with single strut specimen without geometrical shape

After that choose α risk (significant level).

5%: if we are fairly ready to change our minds.

The risk is chosen as 0.05 (5%).

Single strut specimen without geometrical shape (Cylinder), S_1

292.237, 332.295, 289.391, 369.180, 297.813

257.787, 337.909, 328.880, 382.775, 296.205

364.603, 325.976, 306.807, 371.230, 278.503

Calculate mean, X'

$$\begin{aligned}
 X' &= \frac{292.237 + 332.295 + 289.391 + 369.180 + 297.813 + 257.787 + 337.909 + 328.880 + 382.775 + 296.205 + 364.603 + 325.976 + 306.807 + 371.230 + 278.503}{15} \\
 &= \frac{4831.591}{15} \\
 &= 322.106
 \end{aligned}$$

Table 4.4.2.1: Summation on means of Young's modulus for single strut specimen without geometrical shape (Cylinder) F-TEST, S_1

X_i	$X_i - X'$	$(X_i - X')^2$
292.237	-29.869	892.157
332.295	10.189	103.816
289.391	32.715	1070.271
369.180	47.074	2215.961
297.813	-24.293	590.150
257.787	-64.319	4136.934
337.909	15.803	249.735
328.880	6.774	45.887
382.775	60.669	3680.728
296.205	-25.901	670.862
364.603	42.497	1805.995
325.976	3.87	14.977
306.807	-15.299	234.059
371.230	49.124	2413.167
278.503	-43.603	1901.222

From Table 4.4.2.1,

$$\begin{aligned}
 \sum (X_i - X') &= 892.157 + 103.816 + 1070.271 + 2215.961 + 590.150 + 4136.934 \\
 &\quad + 249.735 + 45.887 + 3680.728 + 670.862 + 1805.995 + 14.977 \\
 &\quad + 234.059 + 2413.167 + 1901.222 \\
 &= 20025.921
 \end{aligned}$$

$$S_1 = \sqrt{\frac{20025.921}{14}}$$

$$= 37.821$$

$$S_1^2 = (37.821)^2$$

$$= 1430.428$$

Single strut specimen with geometrical shape (Dogbone2), S_2

171.120, 296.660, 372.960, 214.240, 330.920

331.090, 356.740, 308.190, 280.580, 301.600

315.790, 300.940, 333.160, 334.029, 283.810

Calculate mean, X'

$$X' = \frac{171.120 + 296.660 + 372.960 + 214.240 + 330.920 + 331.090 + 356.740 + 308.190 + 280.580 + 301.600 + 315.790 + 300.940 + 333.160 + 334.029 + 283.810}{15}$$

$$= \frac{4531.829}{15}$$

$$= 302.122$$

Table 4.4.2.2: Summation on means of Young's modulus for single strut specimen with geometrical shape (Dogbone2) F-TEST, S_2

X_i	$X_i - \bar{X}$	$(X_i - \bar{X})^2$
171.120	-131.002	17161.524
296.660	-5.462	296.66
372.960	70.838	5018.022
214.240	-87.882	7723.246
330.920	28.798	829.325
331.090	28.968	839.145
356.740	54.618	2983.126
308.190	6.068	36.821
280.580	-21.542	464.058
301.600	-0.5222	0.272
315.790	13.668	186.814
300.940	-1.182	1.397
333.160	31.038	963.357
334.029	31.907	1018.057
283.810	-18.312	335.329

From Table 4.4.2.2,

$$\begin{aligned} \sum (X_i - \bar{X})^2 &= 17161.524 + 296.66 + 5018.022 + 7723.246 + 829.325 + 839.145 + \\ &\quad 2983.126 + 36.821 + 464.058 + 0.272 + 186.814 + 1.397 + 963.357 \\ &\quad + 1018.057 + 335.329 \\ &= 37857.153 \end{aligned}$$

$$S_2 = \sqrt{\frac{37857.153}{14}}$$

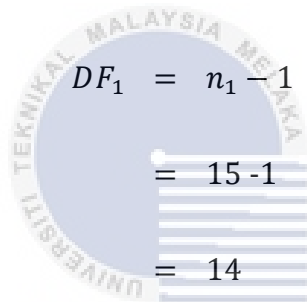
$$= 52.000$$

$$S_2^2 = (52.000)^2$$

$$= 2704$$

F Distributed,

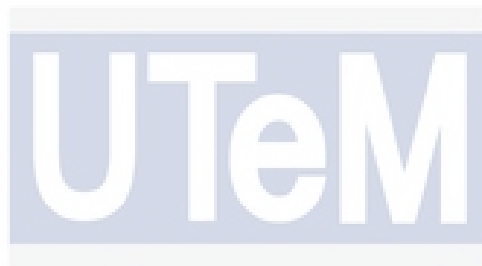
Degree of freedom,



$$DF_1 = n_1 - 1$$

$$= 15 - 1$$

$$= 14$$



Degree of freedom,



$$DF_2 = n_2 - 1$$

$$= 15 - 1$$

$$= 14$$

Based on statement $H_1, \sigma_1 \neq \sigma_2$. Hence, the test is two tail test.

Acceptance region,

$$F > F_{0.975,14,14} = 2.9786$$

$$F < F_{0.025,14,14} = \frac{1}{2.9786}$$

$$= 0.3357$$

$$F_{cal} = \frac{1430.428}{2704}$$

$$= 0.5290$$

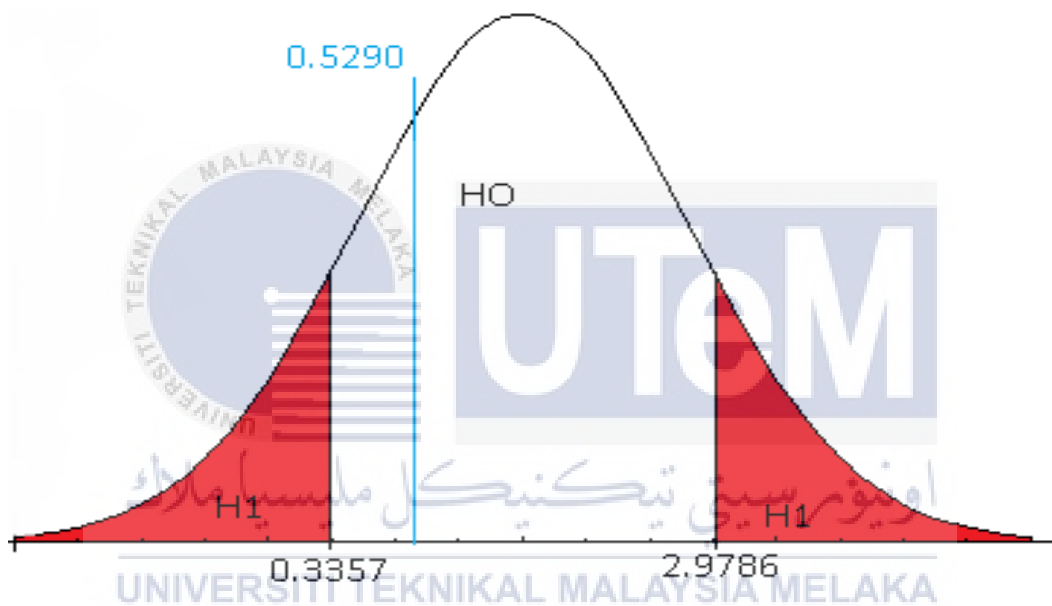


Figure 4.4.2.1: Bell graph for variance at 5% significant level for Cylinder and Dogbone2
(0.48 mm radius fillet)

From Figure 4.4.2.1, engineering conclusion;

Single strut with geometrical shape shows no significant different in variance at 5% significant level.

Comparison of means (t-TEST)

From F-TEST result, $\sigma_1 = \sigma_2$. Therefore formula used for t-TEST is

$$t = \frac{\tilde{x}_1 - \tilde{x}_2}{\sqrt{\frac{1}{n_1} + \frac{1}{n_2}} \sqrt{\frac{(n_1 - 1)s_1^2 + (n_2 - 1)s_2^2}{n_1 + n_2 - 2}}}$$

Where,

$$X'_1 = 322.106 \quad X'_2 = 302.122$$

$$S_1^2 = 1430.428 \quad S_2^2 = 2704$$

$$N_1 = 15 \quad N_2 = 15$$

$H_0 =$ Young Modulus of single strut specimen with geometrical shape is the same with single strut specimen without geometrical shape ($\mu_1 = \mu_2$)

$H_1 =$ Young Modulus of single strut specimen with geometrical shape is the different with single strut specimen without geometrical shape ($\mu_1 < \mu_2$)

$$h_0 : \mu_1 - \mu_2 \geq 0$$

$$h_1 : \mu_1 - \mu_2 < 0$$

Since $h_1 : \mu_1 - \mu_2 < 0$, this is one tail test

$$\text{Where DF} = n_1 + n_2 - 2$$

$$= 15 + 15 - 2$$

$$= 28$$

Acceptance region, H_1

$$t > t_{0.95,28} = 1.701$$

$$t = \frac{322.106 - 302.122}{\sqrt{\frac{1}{15} + \frac{1}{15}} \sqrt{\frac{(15-1)(1430.428) + (15-1)(2704)}{15+15-2}}}$$

$$t = \frac{19.984}{(0.365)(45.467)}$$

$$t = 1.204$$

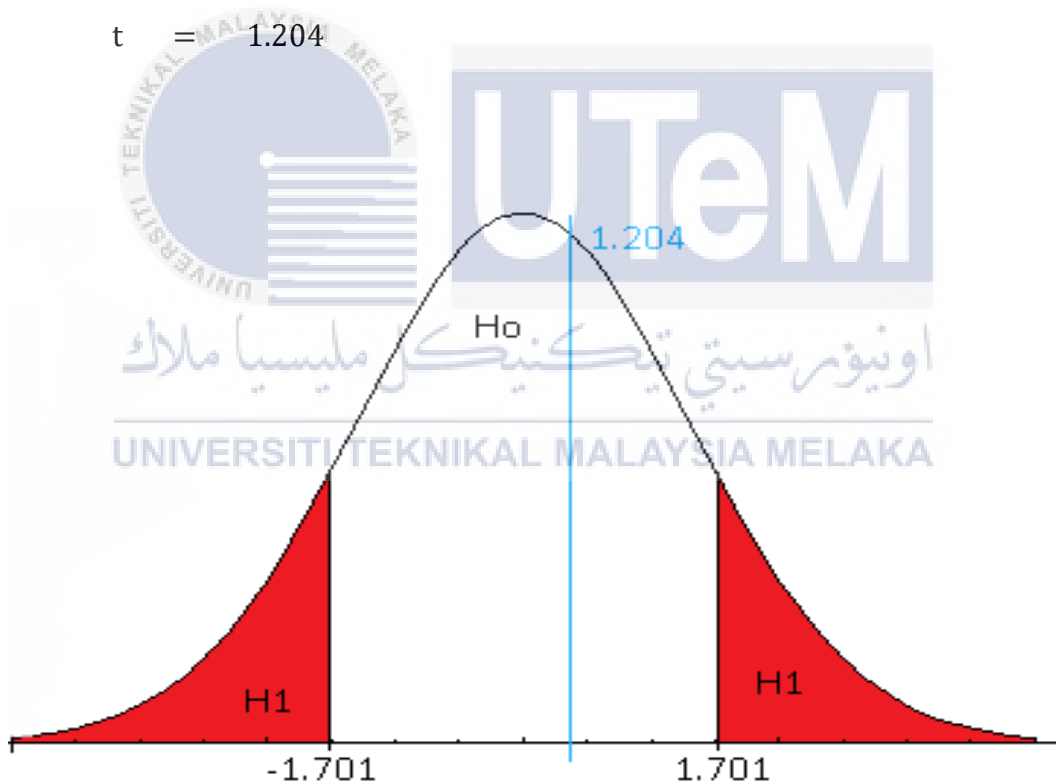


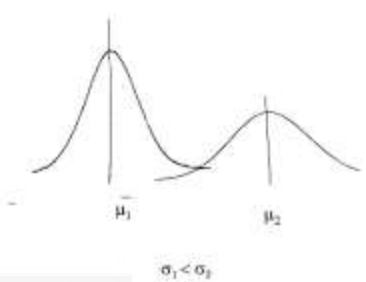
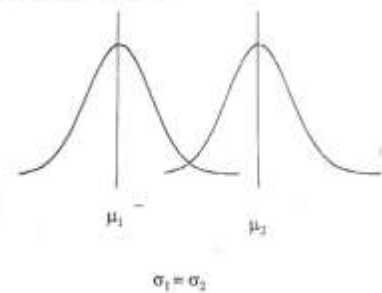
Figure 4.4.2.2: Bell graph for Young's modulus of Cylinder and Dogbone2 (0.48mm radius fillet) t-TEST

From Figure 4.4.2.2, engineering conclusion;

There is insufficient evidence to conclude that single strut with geometrical shape, Dogbone2 has higher Young's modulus values than single strut without geometrical shape.



Table 4.4.2.3: Distribution graph for hypothesis test

Parameter	Engineering Conclusion		Distribution
	F-TEST	t-TEST	
Young's modulus of Cylinder and Dogbone1	Single strut with geometrical shape shows no significant different in variance at 5% significant level.	There is sufficient evidence to conclude that single strut with geometrical shape has higher young modulus than single strut without geometrical shape.	
Young's modulus of Cylinder and Dogbone2	Single strut with geometrical shape shows no significant different in variance at 5% significant level.	There is insufficient evidence to conclude that single strut with geometrical shape, Dogbone2 has higher young modulus than single strut without geometrical shape.	

From Table 4.4.2.3, the Young's modulus values of Cylinder and Dogbone2 has shown insufficient evidence to conclude that single strut with geometrical shape (Dogbone2) has higher Young's modulus than single strut without geometrical shape. Meanwhile for the Young's modulus values of Cylinder and Dogbone1, it is shown from the hypothesis test that there is sufficient evidence to conclude that single strut with geometrical shape has higher young modulus than single strut without geometrical shape.

Table 4.4.2.4: Average Young's modulus mean for single strut specimen with and without geometrical shape

	Single strut specimen without geometrical shape, Cylinder	Single strut specimen with geometrical shape,	
		Dogbone1 (0.9mm radius fillet)	Dogbone2 (0.48mm radius fillet)
Average Young's modulus mean, Mpa	322.106	365.543	302.122

Table 4.4.2.4 shows the average mean values for each single strut. From Table 4.4.2.3 and Table 4.4.2.4, it is shown that single strut specimens with geometrical shape, Dogbone2 do not affect Young's modulus property while single strut specimens with geometrical shape, Dogbone1 do affect the Young modulus property. With this, it is concluded that for miniature tensile test specimen, it does not require geometrical shape for the specimen holder. Simple slender straight design of strut is reliable to be used for miniature tensile test.



CHAPTER 5

CONCLUSION AND RECOMMENDATION

5.1 Conclusion

This study is conducted to assist better understanding on how geometrical shape affects elastic property for lattice structure. Single strut specimens are fabricated with and without geometrical shape. Single strut specimens with geometrical shape are divided into two designs which are single strut with dogbone shape of 0.9mm fillet radius and 0.48mm radius fillet respectively. For single strut specimen without geometrical shape, straight slender cylinder is fabricated. The background of this study is reviewed to gain knowledge and scientific theories that are relevant to this study.

In methodology, single strut specimens are designed by using CAD software which is Solidworks. The designed single strut specimens are then fabricated by using CubePro 3D printer. The fabricated single strut specimens with build angle 35.26° are analysed based on their elastic property after going through tensile test which tested by using Shimadzu EZ Test (EZ-LX) machine. By following workflow chart as a guideline in this study, the results are obtained and discussed.

Three sets of 45 specimens are fabricated successfully by using CubePro 3D printer. Hypothesis test are conducted as a comparative method to analyse the effect of geometrical shape towards the mechanical property. From the result and analysis, it is concluded that for miniature tensile test specimen, it does not require geometrical shape for the specimen holder. Simple slender straight design of strut is reliable to be used for miniature tensile test.

5.2 Recommendation

For future study, tensile test on strut with lattice structure arrangement at the gauge length can be conducted because real case applications are based on lattice structure material. Hence, a comparison can be made between slender straight strut specimen and strut with lattice structure arrangement at the gauge length on their elastic property. By making this comparison, the difference in both performance can be studied and some improvements can be made in order to enhance both performances.



REFERENCES

3D Systems Inc. (2015). CubePro Prosumer 3D printer - User Guide - Original Instructions.

3D Systems, Inc., (September), pp.1–86.

<https://doi.org/10.4337/9781782545583.00006> [Assesed on 2 December 2018].

Augustyniak, M., 2018. Old Material Materials-New Capabilities: Lattice Materials in Structural Mechanics. *J Theoret Appl Mech*, 56(1), pp.213-26.

Calik, A., Sahin, O., and Ucar, N., 2008. Specimen Geometry Effect on the Mechanical Properties of AISI 1040 Steel. *Physical Science*, 63(7–8), pp. 448–452.

Chen, 2018. Study on Single Strut Formation Using Additive Layer Manufacturing Melaka: Universiti Teknikal Malaysia Melaka.

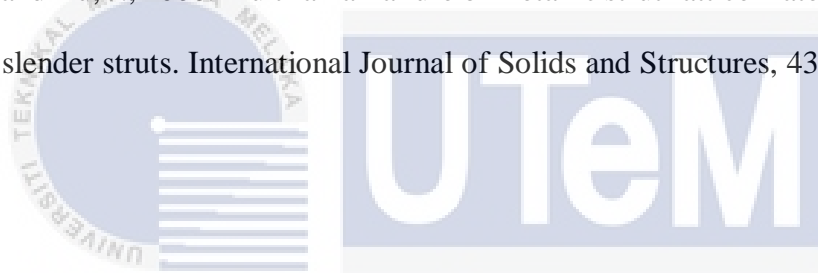
Chen, D. C., You, C. S., Gao, F. Y., 2014. Analysis and Experiment of 7075 Aluminium Alloy Tensile Test, National Changhua University of Education, Taiwan. 11th international Conference on Technology of Plasticity, 19-24 October 2014 at Nagoya Congress Center, Nagoya.

Davami, K., Mohsenizadeh, M., Munther, M., Palma, T., Beheshti, A., and Momeni, K., 2019. Dynamic Energy Absorption Characteristics of Additively-Manufactured Shape-Recovering Lattice Structures. *Materials Research Express*, 6.

Davis, J. R., 2004. *Tensile Testing*, 2nd ed., Ohio: Materials Park.

Davis, J. R., Walter, D. P., Deborah, F. P., 2008. *Peterson's Stress Concentration Factors*, 3rd ed., New York : John Wiley & Sons

Doyoyo, M. and Hu, J., 2006. Multi-axial failure of metallic strut-lattice materials composed of short and slender struts. *International Journal of Solids and Structures*, 43(20), pp. 6115-6139.



Guild, M., Garcia-Chocano, V., Kan, W., and Sanchez-Dehesa, J., 2015. Acoustic Metamaterial Absorbers Based on Multi-layered Sonic Crystal. *Journal of Applied Physics*, 117.

Kessler, J., Bâlc, N., Gebhardt, A., & Abbas, K., 2016. Basic Research on Lattice Structures Focused on the strut shape and welding beads. *Physics Procedia*, 83, pp. 833–838.

Khun, K. and Medlin, D., 2000. *ASM Handbook, Volume 8: Mechanical Testing and Evaluation*, 8th ed., Ohio :Materials Park.

Kilinc, Z., Nava, E., Tyas, A., 2016. Energy Absorption in Lattice Structures in Dynamics. International Journal of Impact Engineering, 89, pp. 49-61.

Kuang K.H., 2007. Statistical Design of Experiment (SDOE), Universiti Teknikal Malaysia, Melaka. Seminar, 6-7 June 2007 at Century Mahkota Hotel, Melaka.

Kumar, P. V., Reddy, G. M. and Rao, K. S., 2015. Microstructure , mechanical and corrosion behavior of high strength AA7075 aluminium alloy friction stir welds e Effect of post weld heat treatment. Defence Technology, 11(4), pp. 362–369.

LaVan, D. A. And Sharpe, W. N., 1999. Tensile Testing of Microsamples. Experimental Mechanics. 39 (3), pp. 210-216

Mines R.A.W., 2008. On The Characterisation of Foam and Micro-lattice Materials Used in Sandwich Construction. Strain, 44(1), pp.71-83.

Mohsenizadeh, M., Gasbarri, F., Munther, M., Beheshti, A., and Davami, K., 2018. Additively-manufactured Lightweight Metamaterials for Energy Absorption. Materials & Design, 139, pp. 521-530.

Rehme, O., Emmelmann, C., 2006. Rapid manufacturing of lattice structures with selective laser melting, Laser-based Micropackaging, 6107, pp. 192-203.

Tan, X., Wang, B., Chen, S., Zhu, S., and Sun, Y., 2019. A Novel Cylindrical Negative Stiffness Structure for Shock Isolation. *Composite Structures*, 214.

Timothy, C.U., 2010. *Statics in Plain English*, 3rd ed., New York: Taylor & Francis Group.

Tsopanos, S., Mines, R.A.W., McKown S., Shen Y., Cantwell W.J., Brooks W., et al., 2010. The influence of processing parameters on the mechanical properties of selectively laser melted stainless steel microlattice structures. *J. Manuf. Sci. Eng.*, pp.132.

Syam, W., Jianwei, W., Zhao, B., Maskery, I., Elmadih, W. and Leach, R. 2017. Design and analysis of strut-based lattice structures for vibration isolation. *Precision Engineering*, 24, pp. 510-523.

Yan, C., Hao, L., Hussein, A., Raymont, D., 2012. Evaluations of Cellular Lattice Structure Manufactured Using Selective Laser Melting. *International J.Mach. Tools Manufacturing*, 62, pp.32-38.

Wahi, A., 2018. Effect of Node Enhancement on Strength of Body-Centered-Cubic (BCC) Polymer Lattice-Structure Material, Melaka: Universiti Teknikal Malaysia Melaka.